



Contents lists available at ScienceDirect

Quaternary Science Reviews

journal homepage: www.elsevier.com/locate/quascirev

Episodic intraplate deformation of stable continental margins: evidence from Late Neogene and Quaternary marine terraces, Cape Liptrap, Southeastern Australia

Thomas Gardner^{a,*}, John Webb^b, Claudia Pezzia^a, Terri Amborn^a, Robert Tunnell^a, Sarah Flanagan^a, Dorothy Merritts^a, Jeffrey Marshall^a, Derek Fabel^c, Matthew L. Cupper^d

^a Keck Geology Consortium, Department of Earth and Environment, Franklin & Marshall College, P.O. Box 3003, Lancaster, PA 17604-3003, USA

^b School of Environmental Science, La Trobe University, Victoria 3086, Australia

^c Department of Geographical and Earth Sciences, East Quadrangle, University of Glasgow, Glasgow G12 8QQ, UK

^d School of Earth Sciences, The University of Melbourne, Victoria 3010, Australia

ARTICLE INFO

Article history:

Received 4 February 2008

Received in revised form

7 October 2008

Accepted 9 October 2008

Available online xxx

ABSTRACT

The Waratah Fault is a northeast trending, high angle, reverse fault in the Late Paleozoic Lachlan Fold Belt at Cape Liptrap on the Southeastern Australian Coast. It is susceptible to reactivation in the modern intraplate stress field in Southeast Australia and exhibits Late Pliocene to Late Pleistocene reactivation. Radiocarbon, optically stimulated luminescence (OSL), and cosmogenic radionuclide (CRN) dating of marine terraces on Cape Liptrap are used to constrain rates of displacement across the reactivated Waratah Fault. Six marine terraces, numbered Qt₆–Tt₁ (youngest to oldest), are well developed at Cape Liptrap with altitudes ranging from ~1.5 m to ~170 m amsl, respectively. On the lowest terrace, Qt₆, barnacles in wave-cut notches ~1.5 m amsl, yielded a radiocarbon age of 6090–5880 Cal BP, and reflect the local mid-Holocene sea level highstand. Qt₅ yielded four OSL ages from scattered locations around the cape ranging from ~80 ka to ~130 ka. It formed during the Last Interglacial sea level highstand (MIS 5e) at ~125 ka. Inner edge elevations (approximate paleo high tide line) for Qt₅ occur at distinctly different elevations on opposite sides of the Waratah Fault. Offsets of the inner edges across the fault range from 1.3 m to 5.1 m with displacement rates ranging from 0.01 mm/a to 0.04 mm/a. The most extensive terrace, Tt₄, yielded four Early Pleistocene cosmogenic radionuclide (CRN) ages: two apparent burial ages of 0.858 Ma ± 0.16 Ma and 1.25 Ma ± 0.265 Ma, and two apparent exposure ages of 1.071 Ma ± 0.071 Ma (¹⁰Be) and 0.798 Ma ± 0.066 Ma (²⁶Al). Allowing for muonic production effects from insufficient burial depths, the depth corrected CRN burial ages are 1.8 Ma ± 0.56 Ma and 2.52 Ma ± 0.88 Ma, or Late Pliocene. A Late Pliocene age is our preferred age. Offsets of Tt₄ across the Waratah Fault range from a minimum of ~20 m for terrace surface trends to a maximum of ~70 m for terrace bedrock straths. Calculated displacement rates for Tt₄ range from 0.01 mm/a to 0.04 mm/a (using a Late Pliocene age, ~2 Ma), identical to the rates calculated for the Last Interglacial terrace, Qt₅. This indicates that deformation at Cape Liptrap has been ongoing at similar time-averaged rates at least since the Late Pliocene. The upper terraces in the sequence, Tt₃ (~110 m amsl), Tt₂ (~140 m) and Tt₁ (~180 m) are undated, but most likely correlate to sea level highstands in the Neogene. Terraces Tt₁–Tt₄ show an increasing northward tilt with age.

The Waratah Fault forms a prominent structural boundary in the Lachlan Fold Belt discernible from airborne magnetic and bouger gravity anomalies. Seismicity and deformation are episodic. Episodic movement on the Waratah Fault may be coincident with sea level highstands since the Late Pliocene, possibly from increased loading and elevated pore pressure within the fault zone. This suggests that intervals between major seismic events could be on the order of 100 ka.

© 2008 Elsevier Ltd. All rights reserved.

1. Introduction

Although Australia is traditionally regarded as a tectonically stable continent (Twidale, 1983), there is a growing realization that several regions of the Australian Craton show evidence for neotectonic activity (Sandiford, 2003). For Southern and Southeastern Australia a rapidly growing body of literature offers rich and robust

* Corresponding author. Department of Geosciences, Trinity University, One Trinity Place, San Antonio, TX 78212, USA. Tel.: +1 210 999 7655; fax: +1 210 999 7090.

E-mail address: tgardner@trinity.edu (T. Gardner).

evidence for “youthful” landscapes (Ollier, 1978; Ollier and Pain, 1994; Quigley et al., 2006; see Bishop, 1998; Sandiford, 2003, for an exceptional summary of these landscapes, their evolution and their tectonic implications). There is compelling evidence from plate reconstructions (Coblentz et al., 1995, 1998; Sandiford, 2003; Sandiford et al., 2004; Nelson et al., 2006; Dyksterhuis and Müller, 2008) that an active phase of deformation, variously termed the Kosciuszko Uplift (Andrews, 1910; Joyce et al., 2003) and Sprigg Orogeny (Sandiford, 2003), began in the Late Miocene to Early Pliocene across a broad section of the Australian continent and is ongoing today. This is demonstrated by contemporary seismicity (Gibson et al., 1981; McCue et al., 1990; Sandiford, 2003; Célérier et al., 2005; Geosciences Australia, Internet Earthquake Database), and a number of structural and geomorphic studies throughout this region (e.g. Bourman and Lindsay, 1989; Murray-Wallace et al., 1996; Sandiford, 2002, 2003; Célérier et al., 2005; Quigley et al., 2006, 2007; Clark et al., in press). Some of the most compelling data on the nature and timing of this active phase of deformation comes from the onshore and offshore geologic record in the Gippsland Basin of Southeastern Australia (Barton, 1981; Hocking, 1988; Bolger, 1991; Dickinson et al., 2002; Holdgate et al., 2003) and the broadly deformed Pliocene and Pleistocene paleo-shorelines in Western Victoria and Eastern South Australia (Sprigg, 1979; Sandiford, 2003; Paine et al., 2004). This phase of Neogene to recent deformation is generally consistent with the modern, intraplate stress field in Southeastern Australia, which is compressive with S_{Hmax} oriented at $130^\circ \pm 20^\circ$ (Hillis and Reynolds, 2003; Sandiford et al., 2004; Nelson et al., 2006) and most likely homogeneous between shallow and seismogenic depths (Clark and Leonard, 2003).

There is an ongoing program to map palaeoseismicity (Gaul et al., 1990) in Australia and assess the current seismic hazards (e.g. Crone and Machette, 1994; Crone et al., 1997, 2003; Clark et al., in press), particularly near major cities, but many of the areas with evidence for recent deformation lack well-defined dating constraints on rates of motion. Furthermore, even where age control is available, many of these studies may not encompass a complete seismic cycle making it difficult to calculate recurrence interval or long-term displacement rate. In particular, few studies have yielded reliable estimates of deformation and seismic activity on specific structures over time periods from Late Pliocene to recent. Thus, there is a clear need for detailed reconstructions of long-term (Late Pliocene to recent) deformation histories along active faults across Australia, that constrain the timing and amount of movement by using a combination of geomorphic, stratigraphic and geochronologic data. This information then needs to be related to the present local stress field to assess the seismic risk in a particular area.

In this paper we present such a study from Cape Liptrap, South-central Victoria, ~150 km southeast of the major population centre of Melbourne. Here, movement along the Waratah Fault, an NE–SW trending reverse fault on the southwest end of the Southeastern Australia Seismic Zone (SESZ) has displaced a flight of six, well developed, Neogene to Holocene marine terraces. Based on differential GPS topographic surveys, detailed stratigraphic descriptions, and geochronologic constraints on terrace ages (using radiocarbon (^{14}C), optically stimulated luminescence (OSL), and cosmogenic radionuclide (CRN) dating), we calculate the amounts, rates, and timing of displacement across the Waratah Fault. We then relate this deformation to the current intraplate stress field to assess the nature of intraplate deformation in stable continental regions (SCR), the potential triggering mechanisms of the faulting, and the current seismic risk in the region.

2. Regional setting

Cape Liptrap (Fig. 1B and C) extends over 10 km southward from the southeast Australian coast, averages about 8 km in width, and is

dominated by a northeast-trending ridge with a maximum elevation of 170 m in the middle of the peninsula. The climate is temperate marine with a mean annual temperature of ~14 °C and mean annual rainfall of ~1 m.

The geology of Cape Liptrap is complex. The basement consists of intensely deformed Paleozoic rocks that form part of the Paleozoic Lachlan Fold Belt, a multi-phased deformation zone of Cambrian to Carboniferous rocks extending roughly north–south through Southeastern Australia (Fig. 1A; Gray, 1988). At Cape Liptrap the Paleozoic basement is comprised of Cambrian greenstones and Ordovician Digger Island Limestone, which are overlain unconformably by the Lower Devonian Waratah Limestone, Liptrap Formation turbidites and Bell Point Limestone (Fig. 1B). Middle Devonian S-type granites intrude this sequence, and are exposed nearby on Wilson Promontory and a small section of the Yanakie Isthmus (Fig. 1B). Cretaceous volcanoclastic rocks rest unconformably on the basement, and are in turn overlain by Tertiary fluvial sediments. Late Tertiary deformation uplifted the Cretaceous rocks along range-bounding faults into major horsts (e.g. the Strzelecki Ranges, north of Cape Liptrap; Fig. 1A), and locally deformed Late Oligocene and Miocene sediments in the Gippsland Basin to the northeast of Cape Liptrap into broad folds and fault-cored monoclines. These elevated structures exhibit up to several hundred metres of erosion prior to deposition of the much less deformed Pliocene Haunted Hill Formation, a unit of coarse-grained alluvial, conglomerates and sandstones (Barton, 1981; Bolger, 1991; Dickinson et al., 2002). Neogene and Quaternary marine, fluvial and aeolian deposits of variable thickness cover much of Cape Liptrap (Gardner et al., 2006), so exposures of underlying basement are limited to coastal outcrops along sea cliffs and beach platforms, incised stream valleys and road outcrops.

The Paleozoic basement at Cape Liptrap is cross-cut by the Waratah Fault, a northeast striking (030°) reverse fault that lies at the southwestern edge of the SESZ (Fig. 1C, inset). The Waratah Fault is a major structural lineament in the region juxtaposing turbidites of the Liptrap Formation on the west against largely Cambrian greenstones on the east. The fault is well exposed in an actively eroding sea cliff on the eastern side of the cape (Fig. 1B). It is composed of 2 parallel strands: one places Waratah Limestone against Bell Point Limestone and the second places Bell Point Limestone against Liptrap Formation turbidites (Sandiford, 1978). A narrow cataclastic zone in the Liptrap Formation marks the fault where it crosses the shoreline at Walkerville South. Where it comes back onshore at Waratah Bay (Fig. 1B), there is a sharp break between an actively eroding bedrock shore platform and sea cliff on the hanging wall, and a broad sandy beach and dunes on the footwall. Along much of its onshore trace, the Waratah Fault is buried by Late Pleistocene and Holocene paleo-dunefields (Gardner et al., 2006) and, from dating in this study, Late Pliocene marine terrace deposits (Fig. 1B). As described in this paper, the rates of Late Pliocene to Late Pleistocene displacement on the Waratah Fault can be determined from geomorphic and geochronologic data on the uplifted marine terraces along Cape Liptrap.

3. Neogene and Quaternary marine terraces – distribution, stratigraphy and age

3.1. Genesis and interpretation of marine terraces

Marine abrasion platforms develop most readily along coastlines when the rate of sea level change approaches zero, so that wave action has sufficient time to erode a seaward sloping surface (Lajoie, 1986; Anderson et al., 1999). The intersection of the marine platform (terrace strath) and the adjacent sea cliff (terrace riser), called the terrace inner edge, approximates a horizontal datum formed near mean high tide (Bradley and Griggs, 1976; Merritts,

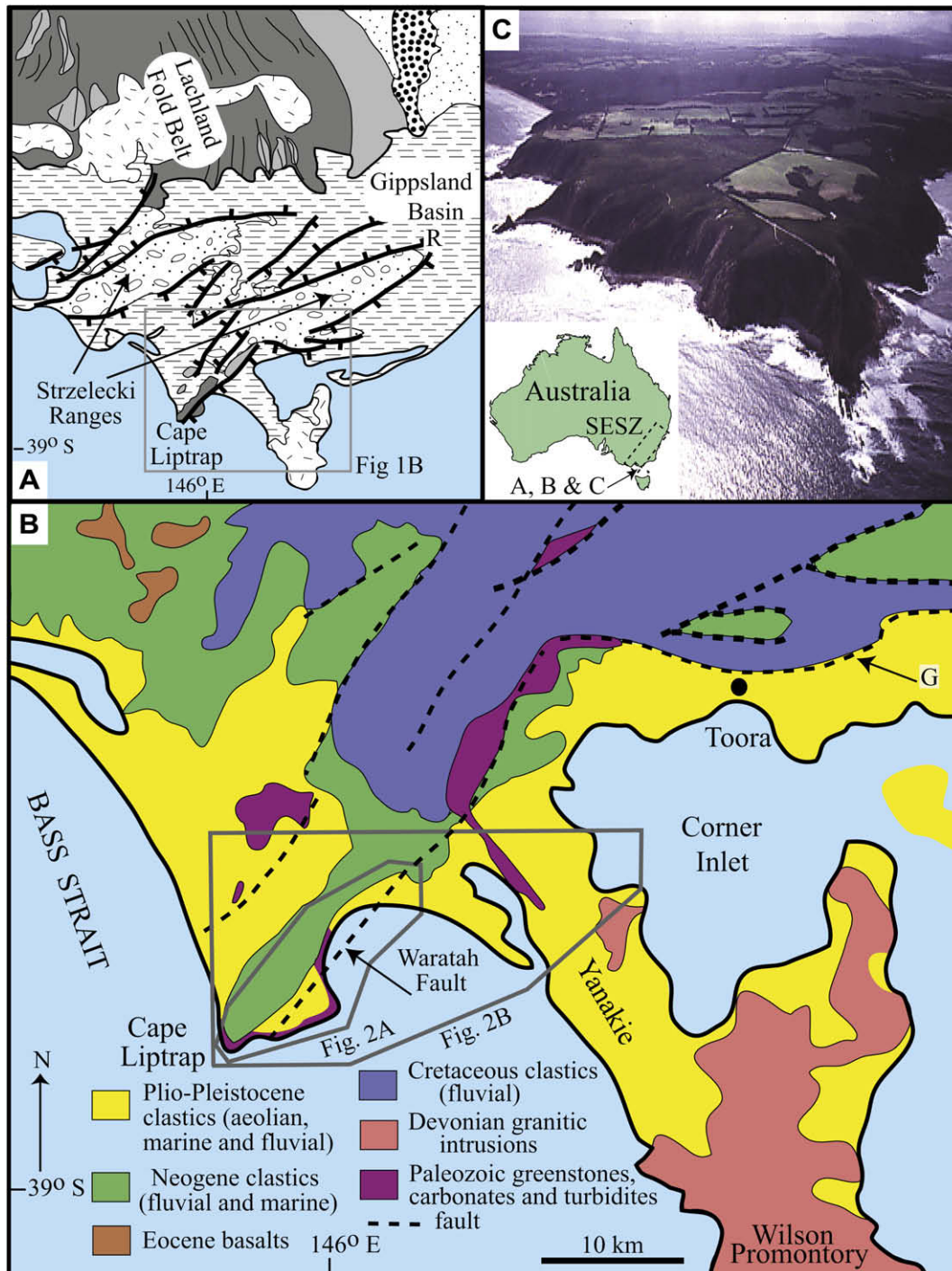


Fig. 1. A) Geologic setting of Cape Liptrap showing the north-south trending Paleozoic Lachlan Fold Belt and the Gippsland Basin with predominately flat lying, but faulted Cretaceous and Tertiary rocks. Thin lines in Lachlan Fold Belt show trend of major folds; heavy lines in Gippsland Basin indicate major range-bounding, reverse faults with ticks on downthrown side. Legend: Ordovician - large dots, Silurian - light gray, Devonian sedimentary rocks - dark gray, Devonian igneous rocks (mostly granites) - hachured, Carboniferous - small dots, Cretaceous - conglomerate, Tertiary - horizontal dashes, ocean - uncolored, R - Rosedale Fault. Modified from Jenkin (1968), Gray (1988), Vandenberg (1988), Geological Survey of Victoria (1993), Vandenberg (1997) and Dickinson et al. (2002). Gray box shows location of B. B) Generalized geologic map for Cape Liptrap and Wilson Promontory. Modified from Douglas and Spencer-Jones (1971), Douglas (1975) and Vandenberg (1997). Polygonal boxes in B show location of Fig. 2A and B. G - Gelliondale Monocline. C) Oblique aerial view of the southern end of Cape Liptrap looking north. Marine terrace T₃ is clearly visible in the cleared fields in the near distance. Dashed diagonal box on inset in C is Southeastern Australia Seismic Zone, SESZ (Sandiford and Egholm, 2008).

1996; Gardner et al., 2001; Kershaw and Guo, 2001; Cooper et al., 2007). Along rocky shorelines, terrace straths are cut into bedrock, and inner edges are easily identifiable at the base of paleo-sea cliffs and often preserved in the landscape, although they may be obscured by colluvium. Bedrock straths may be covered by marine sediment in which case the flat upper surface of the sediment forms the terrace tread.

Marine terraces can form at both sea level maxima (highstands) and minima (lowstands), and are preserved where coastal uplift exceeds the rate of sea level rise or when sea level falls, elevating the sea cliff and marine terrace above the zone of active wave erosion. However, terraces formed at lowstands are rarely preserved, because uplift rates would need to be extremely rapid to elevate the platform above the rising sea level. For example, an

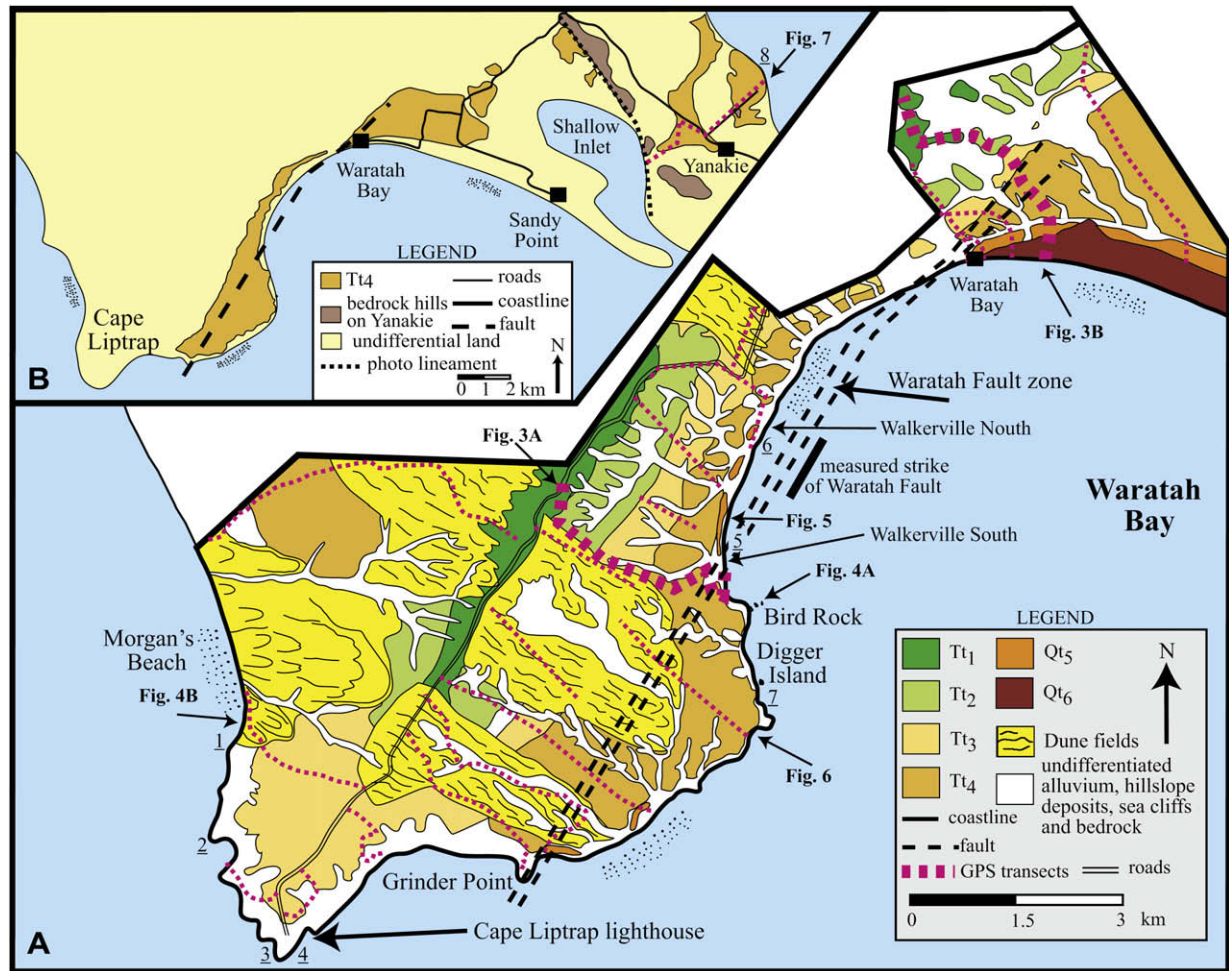


Fig. 2. A) Surficial geologic map of Cape Liptrap showing the distribution of marine terraces. B) Surficial geologic map from the eastern side of Cape Liptrap to the Yanakie Isthmus showing the extent and correlation of Tt₄, Qt₅ and Qt₆ also extend from Cape Liptrap onto the Yanakie Isthmus, but they are generally not visible at the mapping scale. Locations of subsequent figures are shown with arrows. Underlined numbers show locations used in Fig. 8. Dashed lines show location of GPS topographic profiles. Bold dashed lines locate GPS profiles used in construction of cross-sections in Fig. 3. Measured strike of the Waratah Fault in shown by the wide black bar.

uplift rate in excess of 6 mm/a would be required to raise the Last Interglacial lowstand terrace above modern sea level. Thus, exposed marine terraces generally correlate to sea level highstands (i.e. Goy et al., 1992; Merritts, 1996; Perg et al., 2001), especially along relatively stable coastlines like Australia (Murray-Wallace and Belperio, 1991; Stirling et al., 1998; Bourman et al., 1999; Muhs, 2002; Murray-Wallace, 2002).

3.2. Cape Liptrap terraces

A flight of six marine terraces is preserved at Cape Liptrap; from oldest to youngest these are numbered Tt₁–Qt₆. They cover most of the cape, and extend from Morgan's Beach on the west and the Cape Liptrap Lighthouse on the south, past the town of Waratah Bay on the north (Fig. 2A) and eastward across Shallow Inlet onto the Yanakie Isthmus (Fig. 2B). Altogether 21 topographic profiles of varying lengths were measured across the terraces. Elevations with sub-metre accuracy were determined from differentially corrected GPS (coast guard beacon and Optus satellite). Several coastal outcrops were identified that preserve terrace inner edges, especially for Qt₅, providing a superb horizontal datum against which to measure displacements across the Waratah Fault. Elevations for inner edges of Qt₅ and erosional coastal notch elevations for Qt₆ were measured with a rod and level. Stratigraphic columns were measured in sea cliffs from the terrace bedrock strath into the

overlying marine sands, and dated using a combination of radio-carbon, OSL and CRN techniques.

The terraces, which correlate to sea level highstands, range in elevation from ~1.5 m amsl for Qt₆ to ~170 m amsl for Tt₁, the highest elevation on the cape at the local drainage divide (Fig. 3). Terrace trends vary in area and lateral extent (Fig. 2A), from the broadest and most continuous surface, Tt₄, which covers a major portion of Cape Liptrap, to severely eroded trends that preserve only terrace inner edges in modern sea cliffs, as for Qt₅. The thickness of marine sediment overlying the terrace strath surfaces (erosional bedrock unconformities) ranges from >20 m for Tt₄ (Fig. 3B) to <1 m for Tt₁ (Fig. 3B). The terrace strath surfaces are generally not well exposed in the interior of the cape, and the thicknesses of the marine sediments overlying the terrace straths are not well constrained. Late Pleistocene and Holocene aeolian activity (Gardner et al., 2006) has locally reworked the near-surface marine sediments on the terraces into aerially extensive dunefields that cover significant portions of the terrace treads and risers. Locally, terrace risers are also extensively colluviated. However, the nearly flat terrace treads and sloping risers are clearly visible in the field and on stereo aerial photography for all terraces at some locations.

3.2.1. Marine terrace Qt₆

Qt₆ is expressed as a coastal notch in bedrock ~1.5 m above mean sea level (amsl) along the modern shoreline on Cape Liptrap.

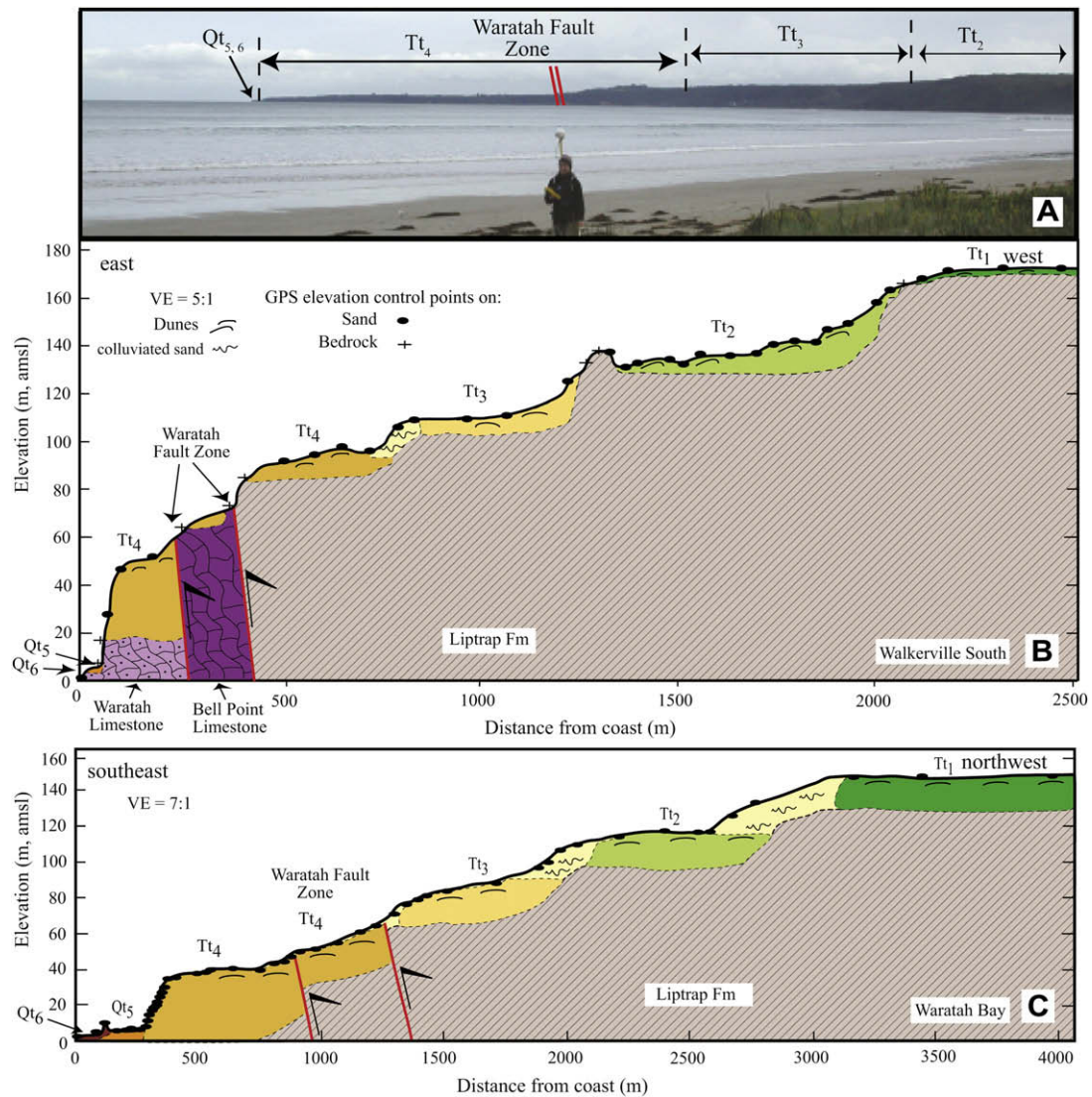


Fig. 3. GPS derived topographic cross-sections showing the distribution and elevation of Late Tertiary and Quaternary marine terraces and bedrock geology; A) photograph looking southwest at Cape Liptrap from Waratah Bay. Marine terrace treads are clearly visible in the skyline. Extent of terrace tread does not exactly match terrace profile in B because the line of the photograph is oblique to the cross-section. B) Terrace flight at Walkerville South. Qt_6 and Qt_5 are projected onto the profile from adjacent GPS transects. C) Terrace flight at Waratah Bay. See Fig. 2 for location of GPS surveys.

At Bird Rock (Fig. 2) a death assemblage of barnacles in growth position occurs in this notch (Fig. 4A). Coastal notches typically form at mean sea level along rocky coastlines from wave action and accelerated weathering (Fischer, 1980; Kershaw and Guo, 2001; Cooper et al., 2007) and a similar notch with living barnacles is currently forming at mean sea level at Bird Rock. The death assemblage of barnacles yielded a mid-Holocene radiocarbon age of 5880 ± 50 a BP (6090–5880 Cal BP, Table 1), slightly older than the age of 5600 a BP obtained from the same barnacles by Haworth et al. (2002). At Waratah Bay, Qt_6 is expressed as a broad, sandy terrace 2–3 m amsl capped by modern dunes (Fig. 2A, Fig. 3C).

The elevation of Qt_6 reflects the mid-Holocene, postglacial relative sea level maximum, which had been recorded at similar elevations around the Australian coast (1.2–3 m, Chappell, 1983; Thom and Roy, 1985; Beaman et al., 1994; Baker et al., 2001; Belperio et al., 2002; Haworth et al., 2002).

3.2.2. Marine terrace Qt_5

Qt_5 is a narrow, but laterally extensive strath terrace eroded into turbidites of the Liptrap Formation. It is best exposed for several hundred metres in a sea cliff at Walkerville North (Fig. 5), where it

is an exceptionally planar surface with centimetre-scale relief. The upper metre of the bedrock strath is deeply weathered. This is quite distinct from the nearby modern wave-cut platform, which exhibits metre-scale relief and a very fresh, unweathered bedrock surface, indicating that the Qt_5 strath represents a longer period of exposure and erosion than the modern platform. At Walkerville North the Qt_5 strath slopes toward the north with a gradient of ~ 0.04 , from an inner edge elevation of 7.25 m amsl at the Waratah Fault to 3.2 m amsl at the north end of the outcrop (Fig. 5A). This gradient is significantly steeper than the average gradient, 0.01–0.02, on the modern, marine abrasion platform on turbidites around Cape Liptrap. Thus, a significant component of the slope of the Qt_5 wave-cut platform is tectonic in origin (discussed further below).

A uniformly thick (0.8 m), marine conglomeratic sand rests on the strath surface at Walkerville North (Fig. 5B and C) and is composed of well-rounded, white pebbles and cobbles of vein quartz (derived from the underlying Liptrap Formation). The clasts are scattered throughout a medium to coarse-grained quartz sand with poorly developed planar and low angle, inclined cross-bedding. The sand was dated to 132 ± 9 ka using OSL (Table 1, OSL-2; Fig. 5C).

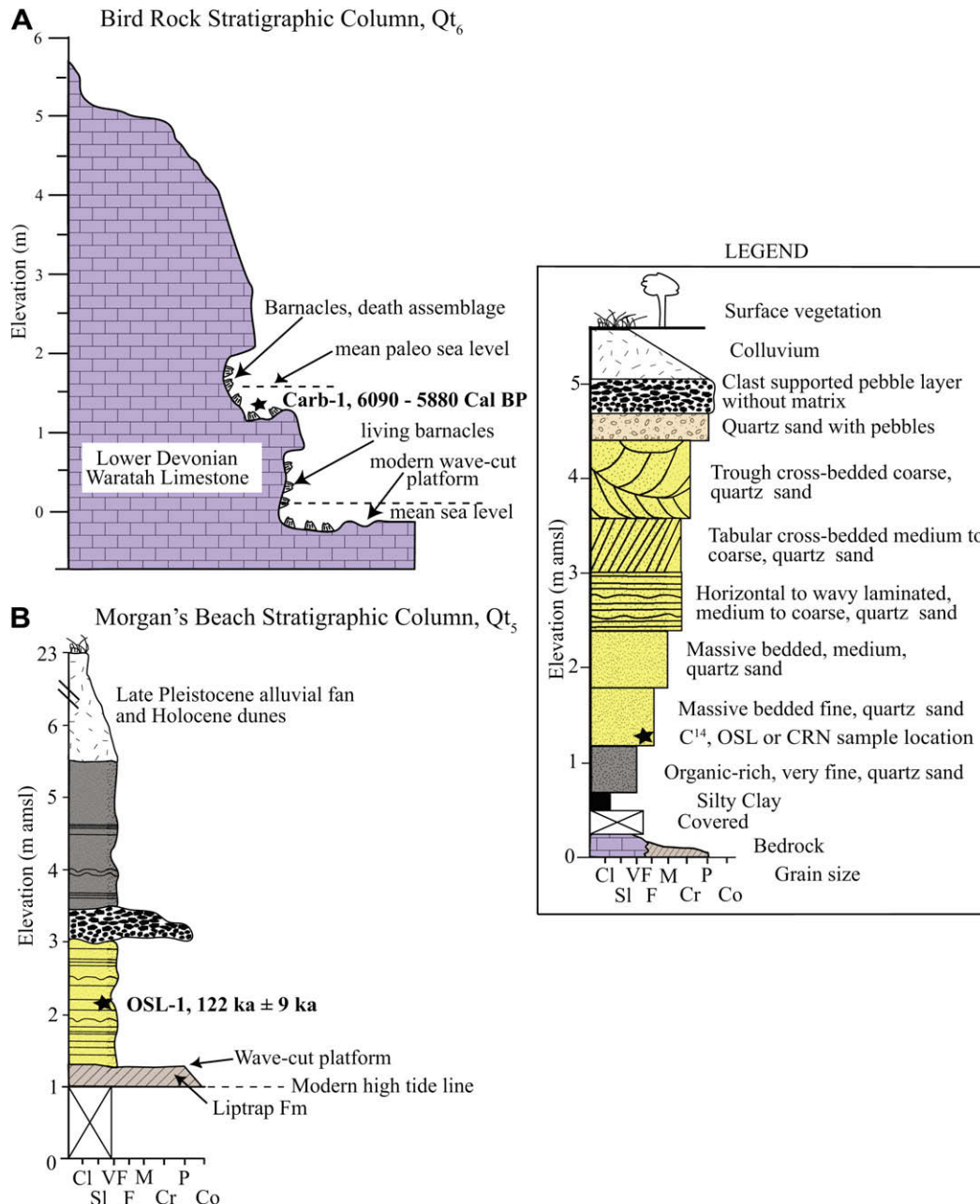


Fig. 4. Stratigraphic columns for A) Qt_6 at Bird Rock, and B) Qt_5 at Morgan Beach. Legend refers to Figs. 4–7. All grain sizes determined by comparison to grain size chart. Cl = clay; Sl = silt; VF = very fine sand, F = fine sand; M = medium sand; Cr = coarse sand; P = pebbles; Co = cobbles. See Fig. 2 for location.

Qt_5 is also well exposed at Morgan's Beach (Fig. 4B) at an elevation of 1.2 m amsl. The outcrop here is not an inner edge, but lies several 10s of metres seaward of the paleo-sea cliff. The strath is overlain by a ~4 m thick, horizontal to wavy bedded, fine to very fine-grained, well sorted, rounded quartz sand, organic rich near the top (Gardner et al., 2006), dated as 122 ± 9 ka (Table 1, OSL-1; Fig. 4B). Lenses up to 0.5 m thick of angular sandstone pebble and cobbles occur locally and are derived from the Liptrap Formation exposed in the paleo-sea cliff.

At Tracy's Beach (Fig. 6A, B) the inner edge of Qt_5 is exposed at an elevation of 2.1 m amsl, and the marine sediment on the strath is ~1.2 m thick. It consists of a lower coarse sand unit with quartz pebbles and cobbles, and an upper medium to coarse sand unit indurated with iron cement. It yielded an OSL age of 122 ± 13 ka (Table 1, OSL-4; Fig. 6A).

Qt_5 is poorly exposed at Walkerville North Campground (Fig. 2A, location 6) at an elevation of 4.5 m amsl. Scattered, well-rounded,

white vein quartz pebbles and cobbles occur on the strath surface in a very thin sand unit. Aeolian sediment on the strath surface yielded an OSL age of 79 ± 6 ka (Table 1, OSL-3). At ~80 ka there was very intense aeolian activity on the west side of Cape Liptrap (Gardner et al., 2006). These dunefields evidently migrated across the cape and buried the Qt_5 platform at Walkerville North Campground.

Qt_5 is expressed as a broad marine terrace at 4–6 m amsl along the coast east from the town of Waratah Bay (Fig. 2A, Fig. 3C). It is locally covered by Holocene dunes.

The OSL ages for Qt_5 at Cape Liptrap are consistent with the Last Interglacial highstand (MIS 5e), which has been dated around Australia as 125 ± 5 ka, and is the best represented of the MIS 5a/c/e marine terraces along the Australian coastline (Murray-Wallace and Belperio, 1991; Stirling et al., 1998; Muhs, 2002). The elevation of the MIS 5e highstand ranges from ~2 m amsl for the stable

Table 1

Radiocarbon, optically stimulated luminescence, and cosmogenic radionuclide ages for samples at Cape Liptrap.

Radiocarbon ages ^a																			
Sample ID	Australian map grid zone 55		Measured radiocarbon age		¹³ C/ ¹² C ratio		Conventional radiocarbon age ^b		2 Sigma calibration										
Qt ₆ -Carb-1 Beta 16980 AMS	413900E/569800N		5140 ± 40 BP		+1.3 o/oo		5580 ± 50 BP		Cal BP 6090–5880										
Optically stimulated luminescence ages ^c																			
Sample ID	Australian map grid zone 55	Depth ^d (m)	Water ^e (%)	⁴⁰ K ^f (Bq kg ⁻¹)	²²⁸ Th ^f (Bq kg ⁻¹)	²²⁸ Ra ^f (Bq kg ⁻¹)	²³⁸ U ^f (Bq kg ⁻¹)	²²⁶ Ra ^f (Bq kg ⁻¹)	²¹⁰ Pb ^f (Bq kg ⁻¹)	K ^g (%)	Th ^g (ppm)	U ^g (ppm)	α radiation ^h (Gy ka ⁻¹)	β radiation ⁱ (Gy ka ⁻¹)	γ radiation ^j (Gy ka ⁻¹)	Cosmic-ray radiation ^k (Gy ka ⁻¹)	Total dose rate (Gy ka ⁻¹)	Equivalent dose ^l (Gy)	Optical age (ka)
Qt ₅ -OSL-1	405800E/5696900N	20.2	33.0 ± 5.0	107.3 ± 2.3	10.0 ± 0.2	9.8 ± 0.2	10.0 ± 0.5	8.0 ± 0.2	8.8 ± 0.6	na	na	na	0.03 ± 0.01	0.30 ± 0.02	0.21 ± 0.01	0.02 ± 0.01	0.56 ± 0.03	68 ± 3	122 ± 9
Qt ₅ -OSL-2	412800E/5698900N	4.0	2.5 ± 1.0	na	na	na	na	na	na	0.43 ± 0.03	4.1 ± 0.2	0.8 ± 0.1	0.03 ± 0.01	0.51 ± 0.03	0.64 ± 0.05	0.11 ± 0.02	1.29 ± 0.06	170 ± 7	132 ± 8
Qt ₅ -OSL-3	413100E/5700200N	6.0	2.5 ± 1.0	na	na	na	na	na	na	1.19 ± 0.06	8.1 ± 0.4	1.9 ± 0.2	0.03 ± 0.01	1.29 ± 0.07	0.65 ± 0.05	0.08 ± 0.02	2.04 ± 0.10	162 ± 8	79 ± 6
Qt ₅ -OSL-4	432500E/5706900N	1.9	2.5 ± 1.0	27.1 ± 1.8	15.1 ± 0.2	15.4 ± 0.6	8.0 ± 3.5	8.5 ± 0.3	5.7 ± 1.6	na	na	na	0.03 ± 0.01	0.23 ± 0.02	0.25 ± 0.01	0.17 ± 0.02	0.68 ± 0.04	83 ± 9	122 ± 13
Cosmogenic radionuclide ages ^m																			
Sample ID	Australian map grid zone 55	Elevation ⁿ (m amsl)	Burial depth (m)	[¹⁰ Be] ^o (×10 ⁵ at/g)	[²⁶ Al] ^o (×10 ⁵ at/g)	[²⁶ Al]/[¹⁰ Be]	Apparent burial age ^p (Ma)	Apparent ¹⁰ Be exposure age (Ma)	Apparent ²⁶ Al exposure age (Ma)	Depth corrected burial age ^q (Ma)									
Qt ₄ -COS-1	413500E/5696800N	25	11	0.52 ± 0.04 (B1275)	1.81 ± 0.38 (A0803)	3.5 ± 0.8	1.125 ± 0.271	na	na	2.52 ± 0.88									
Qt ₄ -COS-2	432200E/5707400N	9	5	0.95 ± 0.12 (B1276)	3.73 ± 0.45 (A0804)	3.9 ± 0.7	0.858 ± 0.166	na	na	1.87 ± 0.56									
Qt ₄ -COS-3	432200E/5707400N	14	0	39.8 ± 1.1 (B1274)	160.1 ± 9.1 (A0813)	4.0 ± 0.3	0.070 ± 0.007	1.071 ± 0.071	0.798 ± 0.066										

^a Beta Analytic Inc., Miami, Florida.^b Corrected for marine reservoir effects.^c OSL analyses performed at the Luminescence Dating Facility, School of Earth Sciences, Melbourne University. Samples were dated using a single-aliquot regenerative-dose (SAR) protocol (Murray and Roberts, 1998; Murray and Wintle, 2000) applied to small (5–10) grain aliquots of 90–125 μm size-fraction quartz. Analytical procedures are described in Cupper (2006).^d Depth measured from Figs. 4, 5, and 7.^e Estimated time-averaged moisture contents, based on measured field water values (% dry weight).^f Obtained by high-resolution gamma spectrometry (HRGS; CSIRO Land and Water, Canberra).^g Obtained by instrumental neutron activation analysis (INAA; Becquerel Laboratories, Mississauga).^h Assumed internal alpha dose rate.ⁱ Derived from INAA radionuclide concentrations (OSL-2, OSL-3) or HRGS radionuclide activities (OSL-4, OSL-1) using the conversion factors of Adamec and Aitken (1998), corrected for attenuation by water and beta attenuation.^j Derived from field gamma spectrometry measurements (OSL-2, OSL-3) or HRGS (OSL-4, OSL-1) using the conversion factors of Adamec and Aitken (1998), corrected for attenuation by water.^k Calculated using the equation of Prescott and Hutton (1994), based on sediment density, time-averaged depth and site latitude and altitude.^l Including a ±2% systematic uncertainty associated with calibration of the laboratory beta-source.^m Samples were measured at the ANTARES AMS Facility at ANSTO, Australia (Fink et al., 2004).ⁿ Elevation and burial depth are measured from stratigraphic columns in Figs. 6 and 7.^o Concentrations at site location with AMS cathode No. in brackets. Samples were measured at the ANTARES AMS Facility at ANSTO, Australia (Fink et al., 2004). Uncertainty represents quadrature addition of 1σ errors in final AMS isotope ratio, masses, Al assay and a 2% systematic variability in repeat measurement of AMS standards.^p Burial ages are calculated according to Granger and Muzikar (2001) with altitude and latitude scaling factors calculated according to Stone (2000) using sea level high latitude production rates of 5.1 ± 0.3 at/g/year and 31.1 ± 1.9 at/g/year for ¹⁰Be and ²⁶Al respectively (Stone, 2000). The burial ages are minimum ages given insufficient burial depth to completely shield samples from cosmic radiation, especially muonic production effects.^q Depth corrected burial age calculated according to Granger and Muzikar (2001) accounting for muonic production given constant sample burial depths and an assumed sediment density is 2 g/cm³.

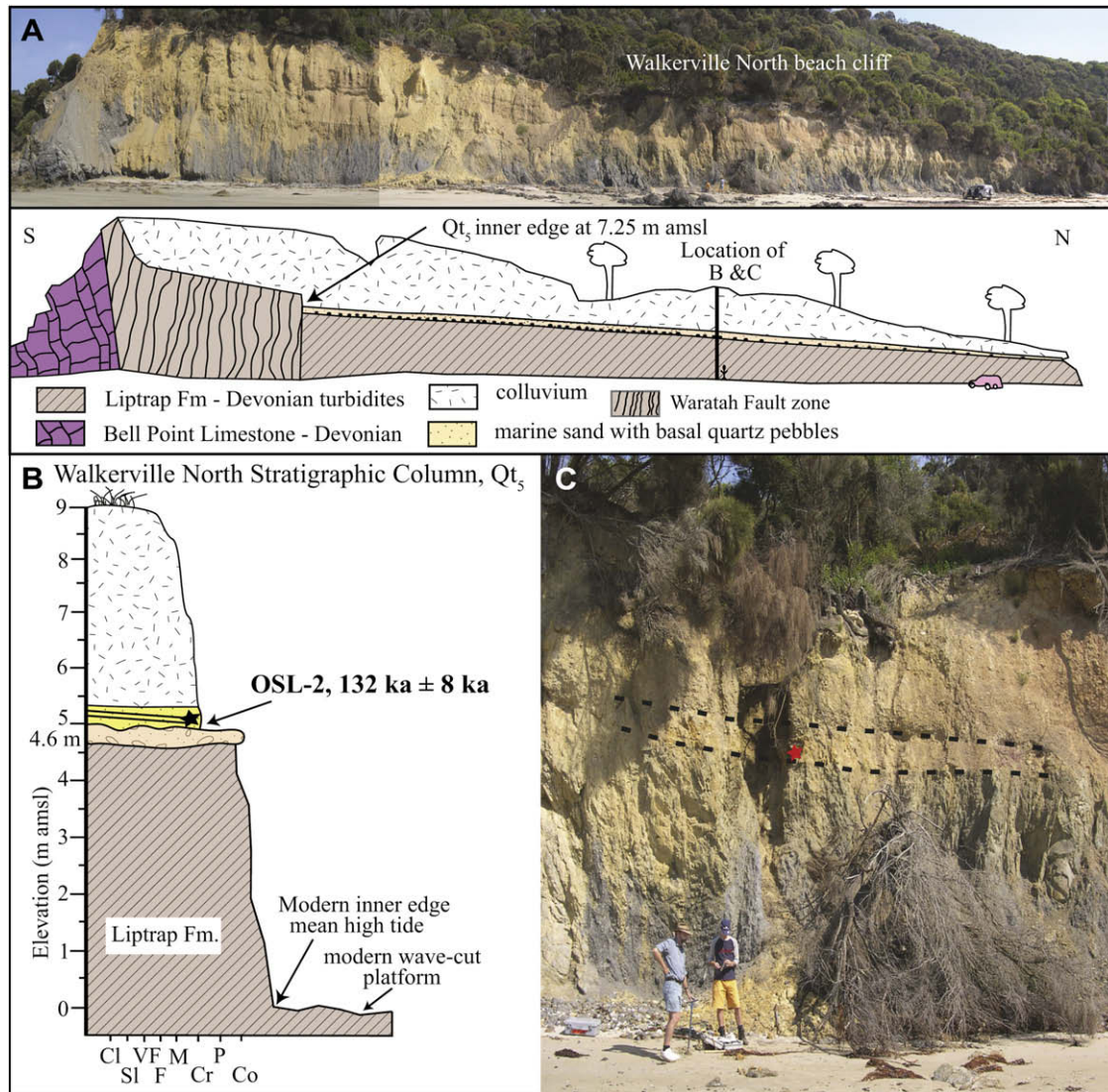


Fig. 5. A) Composite photograph and line drawing of the Walkerville North sea cliff showing the well-developed Qt_5 strath surface on the Liptrap Formation, marine sediment, overlying colluvium and intersection with the Waratah Fault. View is to the west. Truck on right side gives scale. Scale for line drawing and photograph are identical. Geology of the Waratah Fault from Sandiford (1978). B) Stratigraphic column of Qt_5 at Walkerville North. C) Photograph of OSL sample site. See Fig. 2 for location.

Precambrian Gawler Craton on the Eyre Peninsula, South Australia (Murray-Wallace and Belperio, 1991; Bourman et al., 1999; Murray-Wallace, 2002) to ~3 m for the stable coastline of Western Australia (Stirling et al., 1998). The substantial range in elevation for Qt_5 over short distances at Cape Liptrap (1.2–7.25 m amsl) reflects neotectonic activity, which is discussed in detail below.

3.2.3. Marine terrace Tt_4

Tt_4 is the most continuous and aerially extensive marine terrace on Cape Liptrap (Fig. 2). It can be traced nearly continuously from Grinder Point (Fig. 2A) to the Yanakie Isthmus (Fig. 2B). It is well exposed in sea cliffs at North Tracy's Beach on the Yanakie Isthmus (Fig. 6C) and at Digger Island on Cape Liptrap (Fig. 7). The terrace tread is exceptionally flat, although this is obscured where it is buried by Late Pleistocene and Holocene dunefields (Fig. 2A). On the downthrown (Southeastern) side of the Waratah Fault, Tt_4 has a gradual northwards gradient of ~0.0014, decreasing ~10 m in elevation from ~50 m amsl at Walkerville South (Fig. 3B) to ~40 m amsl at Waratah Bay (Fig. 3C). On the upthrown side of the fault, the tread elevation is ~90 m amsl at Walkerville South (Fig. 3B), but the gradient is difficult to estimate because the terrace tread is extensively colluviated and covered by aeolian deposits at Waratah Bay.

Tt_4 is covered by thick, fine to coarse-grained, quartzose sands with granules and pebbles of milky-white vein quartz and smoky-gray granitic quartz; the latter was probably derived from granite on Wilson Promontory. Pebble-rich sands at the base of the sequence fine upwards to medium and fine sand beds at the top. One light brown, silty clay bed is present near the top of the section. Bedding ranges from massive to low angle, bi-directional, tangential and tabular or trough cross-bedding. Intraformational rip-up clasts of brown clay occur in several beds in the middle of the section. On the east side of Cape Liptrap these sands are thicker than on any of the other terraces, and range from >20 m thick on the downthrown side of the Waratah Fault both at Walkerville South (Fig. 3B) and in the well-exposed section in the sea cliff at Digger Island (Fig. 7), to <10 m thick on the upthrown side of the fault at Walkerville South (Fig. 3B). This difference in sediment thickness across the fault probably reflects tectonic movement contemporaneous with deposition (as discussed later), although there may be some influence from seaward depositional thickening. Because the terrace surface is entirely covered by sediment, no inner edges can be recognised. On the west side of Cape Liptrap, aeolian activity deflated nearly all marine sediments on Tt_4 , leaving only isolated, Late Pleistocene dunes on the strath surface (Gardner et al., 2006).

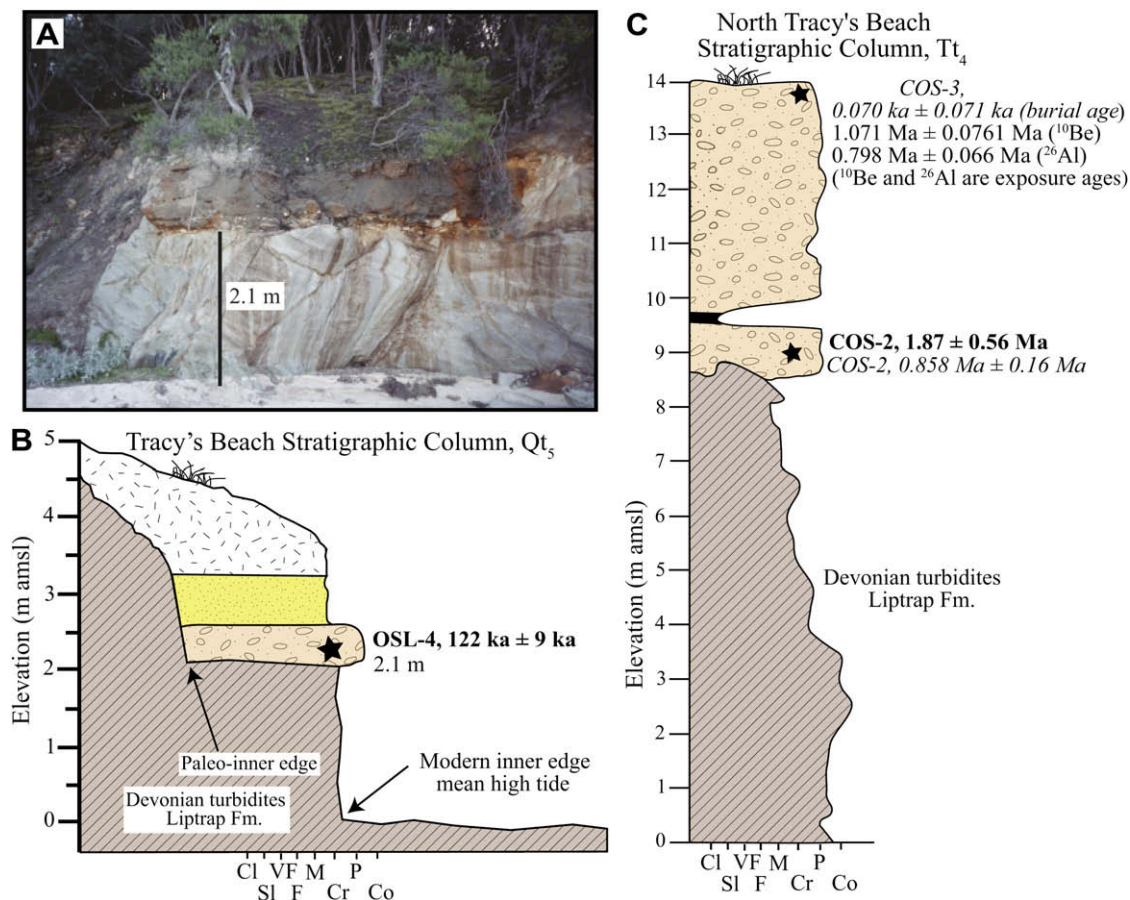


Fig. 6. A) Photograph and (B) stratigraphic column of Qt₅ at Tracy's Beach. C) Stratigraphic column of Tt₄ at North Tracy's Beach. Depth corrected CRN burial ages in bold type and apparent CNR burial ages in italics. See Fig. 2 for location.

Outcrops of Tt₄ yielded two cosmogenic radionuclide apparent burial ages of 1.125 ± 0.265 Ma (Table 1, COS-1; Fig. 7, Digger Island) and 0.858 ± 0.16 Ma (Table 1, COS-2; Fig. 6, North Tracy's Beach). Additionally, a surface sample from North Tracy's Beach gave an apparent ¹⁰Be exposure age of 1.071 ± 0.071 Ma, an apparent ²⁶Al exposure age of 0.798 ± 0.066 Ma, and an apparent burial age of 70 ± 9 ka (Table 1, COS-3). The burial ages are minimum ages because the burial depth is insufficient to completely shield samples from cosmogenic radiation, especially muonic production effects. Allowing for muonic production at the specified burial depth, Tt₄ is 1.87 ± 0.56 Ma at North Tracy's Beach and 2.52 ± 0.88 Ma at Digger Island (Table 1). The depth corrected ages are the more reliable ages and our preferred ages because the samples were definitely not buried deeply enough to shield them from muons. The assumption in the depth corrected calculation is that the burial depth has not changed. This assumption is supported by the low surface erosion indicated by the old surface exposure age for COS-3. Both depth corrected CRN burial ages overlap within the range of statistical uncertainty.

Thus, Tt₄ represents a very extensive marine terrace of Late Pliocene age. It most likely formed during a Late Pliocene sea level highstand (Haq et al., 1987; Dowsett and Cronin, 1990; Pazzaglia and Gardner, 1993; Kotsonis, 1996; Kominz et al., 1998). At this time the warm Early to mid-Pliocene climates with higher eustatic sea levels changed to the cooler Late Pliocene and Quaternary climates with lower sea levels and greater amplitude of eustatic variations. This change is postulated to control the disconformable relationship between Pliocene and Quaternary shoreline deposits in Southeastern Australia (Wallace et al., 2005) and most likely controlled the change from well developed and preserved Late

Pliocene to poorly developed and poorly preserved Quaternary marine terraces at Cape Liptrap. Even the Last Interglacial (MIS 5e) highstand terrace, Qt₅, is only locally preserved with a thin, marine sediment cover along its most landward portion. The poor preservation of Quaternary terraces may reflect a significant change in the tectonic regime, sediment supply and geographically controlled wave climate in Waratah Bay since the Late Pliocene.

We propose that Tt₄ is the marine equivalent of the fluvial Haunted Hill Formation in the Gippsland Basin to the north. In the Gippsland Basin the Haunted Hill Formation contains Pliocene palynomorphs (summarized in Dickinson et al., 2002) and unconformably overlies the Jemmy Point Formation, which has yielded a strontium isotopic age of 2.5–3.5 Ma and a foraminiferal age of 3.2–4.5 Ma in east Gippsland (Wallace et al., 2005).

3.2.4. Marine terraces Tt₃, Tt₂ and Tt₁

Around Cape Liptrap the three high level terraces Tt₃, Tt₂ and Tt₁ occur as well defined, planar treads separated by distinct risers (Figs. 2 and 3), typical of the stair-step topography of coastal marine terraces around the world. Tt₃, Tt₂ and Tt₁ extend from the southern tip of Cape Liptrap to north of Waratah Bay and beyond the mapped area. Tt₃ is the most aerially extensive of the three and is especially well expressed north of the Cape Liptrap lighthouse (Fig. 1C and Fig. 2A). The exposed strath surfaces are eroded into deformed turbidities of the Liptrap Formation and have very little topographic relief. Where exposed the bedrock surface has been extensively mechanically weathered, probably during the dry, cold conditions in the Late Pleistocene (Gardner et al., 2006). Along the southern and western side of the cape and along the highest elevations at the drainage divide, the Tt₁ tread has been completely

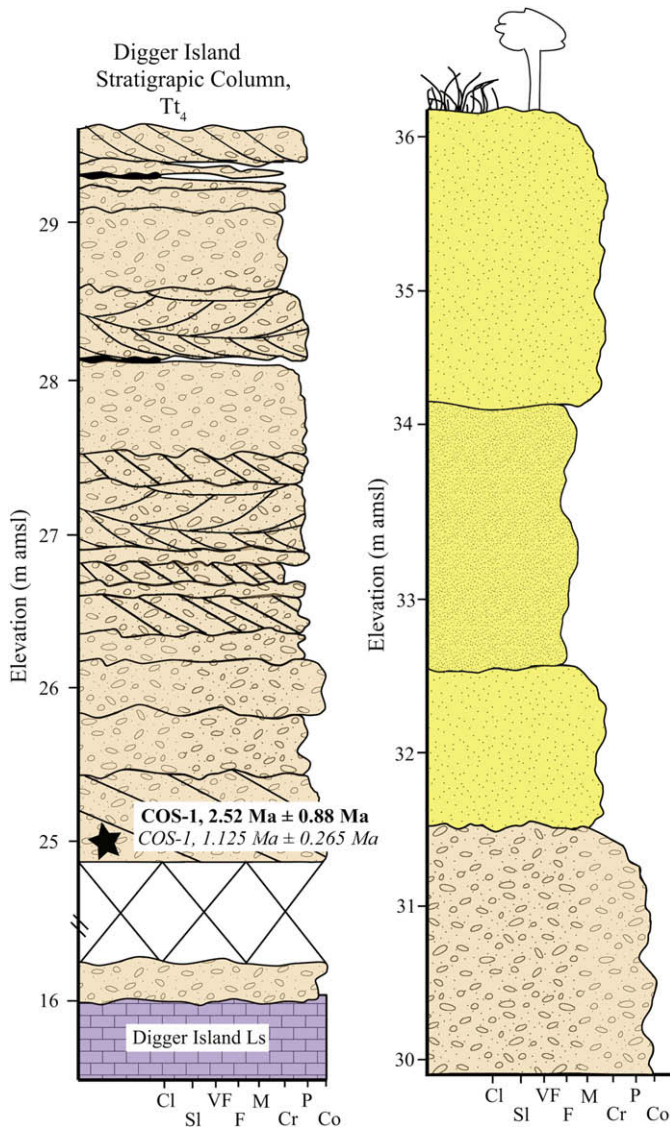


Fig. 7. Stratigraphic column for Tt₄ at Digger Island. Depth corrected CRN burial ages in bold type and apparent CRN burial ages in italics. See Fig. 2 for location.

deflated by aeolian processes and is littered with a lag of rounded to sub-rounded quartz pebbles and cobbles some of which are not derived from the underlying bedrock. Deflation has occurred locally on the Tt₃ and Tt₂ treads as well. Along the eastern side of Cape Liptrap the Tt₃, Tt₂ and Tt₁ treads are buried by extensive Late Pleistocene and Holocene dunefields (Fig. 2).

At Waratah Bay, the marine sediments on Tt₃, Tt₂ and Tt₁ are greater than 20 m thick, but exposures are poor, often colluviated and the strath surfaces are not well exposed. The sediments consist of thick, fine to coarse-grained, quartzose sands with granules and pebbles of milky-white vein quartz and smoky-gray granitic quartz which was probably derived from granite on Wilson Promontory. The sequence fines upwards to medium and fine sand beds at the top, similar to marine sediments on Tt₄. Bedding ranges from massive to low angle, bi-directional, tangential and tabular or trough cross-bedding.

Terrace treads of Tt₃, Tt₂ and Tt₁ are tilted to the northeast, with the oldest terrace showing the greatest tilt. Tt₁ has a gradient of ~ 0.004 , decreasing 30 m in elevation from ~ 170 m amsl at Walkerville South (Fig. 3B) to ~ 140 m amsl at Waratah Bay (Fig. 3C). In comparison, Tt₂ and Tt₃ have gradients of ~ 0.003 , their elevations dropping only ~ 20 m over the same distance (Fig. 3B and C). By

comparison, Tt₄ has a northwards gradient of ~ 0.0014 (as previously discussed). Thus, amount of regional tilting consistently increases with terrace elevation and age, except for Qt₅ where the locally higher slope, 0.04 results from tilting within strands of the Waratah Fault at Walkerville North (Fig. 5A). Terraces Tt₃, Tt₂ and Tt₁ occur only on the northwestern (upthrown) side of the Waratah Fault and are not useful for estimating displacements across this fault.

Terraces Tt₃, Tt₂ and Tt₁ must be older than Tt₄ (Late Pliocene) but cannot be dated more precisely with CRN because of the very poor exposures and complex history of aeolian and colluvial burial and exposure of the marine sediments. Well-developed terraces of similar elevation have been mapped along coastal portions of the Gippsland Basin, 50–250 km northeast of Cape Liptrap (Douglas, 1972, 1993; VandenBerg, 1977, 1997), with the highest terrace (180 m) assigned a Pliocene age (Ward et al., 1971; Ward, 1985), but this is not well constrained (Jenkin, 1968, 1988) and some of these terraces could be fluvial (Jenkin, 1981). Young and Bryant (1993) assigned the highest marine terrace along the southern New South Wales coast to the Neogene, although this is much lower in elevation (25–30 m amsl) than the older Cape Liptrap terraces. Given the uncertainty in age for Tt₃, Tt₂ and Tt₁ at Cape Liptrap, they are here assigned only a broadly Neogene age.

4. Discussion

4.1. Magnitudes and rates of deformation

Deformation on the Waratah Fault can be constrained by displacements of the two marine terraces, Qt₅ and Tt₄, which are cut by the fault. Offsets of inner edges of Qt₅ across the Waratah Fault range from 1.3 m to 5.1 m (Fig. 8A). The maximum value is the difference between the highest inner edge elevation on the upthrown side at Walkerville North Beach Cliff (Fig. 5B) and the lowest inner edge elevation on the downthrown side at Tracy's Beach (Fig. 6B). The minimum value is the difference between the lowest elevation on the upthrown side at Walkerville North Campground and the highest elevation on the downthrown side at Maitland Beach. The differences in elevation of the inner edge on the upthrown side reflect scissor movement along the fault, tilting the terrace toward the north (Fig. 5A). Using an age of ~ 125 ka for Qt₅, displacement rates along the Walkerville sections range from 0.01 mm/a in the north to 0.04 mm/a in the south (Fig. 8A).

Displacement of Tt₄ across the Waratah Fault is substantial, but because of a complete lack of inner edge exposures, has to be calculated from either the surface of the sediment covering the terrace (tread) or the underlying bedrock strath. Both the strath and the tread of the terrace have a seaward slope, making it difficult to identify an exactly equivalent point on either side of the fault, so the calculated offsets will have inherent variability. Maximum offset (Fig. 8B) of Tt₄ across the Waratah Fault is ~ 70 m, using elevation differences between the bedrock straths at Walkerville South (~ 80 m amsl, Fig. 3B) and Tracey's Beach North (8.9 m amsl, Fig. 6B). The terrace straths on opposite sides of the fault at Walkerville South are displaced 65 m (Fig. 3B), but here the terrace treads are offset only ~ 45 m, reflecting the different sediment thicknesses covering the strath on either side of Waratah Fault, probably due to syndepositional fault movement. At Waratah Bay there are no exposures of the Tt₄ bedrock strath, but the terrace tread is well developed, separated from Qt₅ and Tt₃ by distinct colluviated risers, and offset only ~ 20 m (60 m amsl on the upthrown side and 40 m amsl on the downthrown side; Fig. 3C, Fig. 9B). The northwards decrease in tread displacement from ~ 45 m to ~ 20 m is consistent with the northward tilt of the treads of the older Tt₃, Tt₂ and Tt₁ terraces and the strath of the younger Qt₅ terrace. The youngest terrace, Qt₆, does not show this tilting.

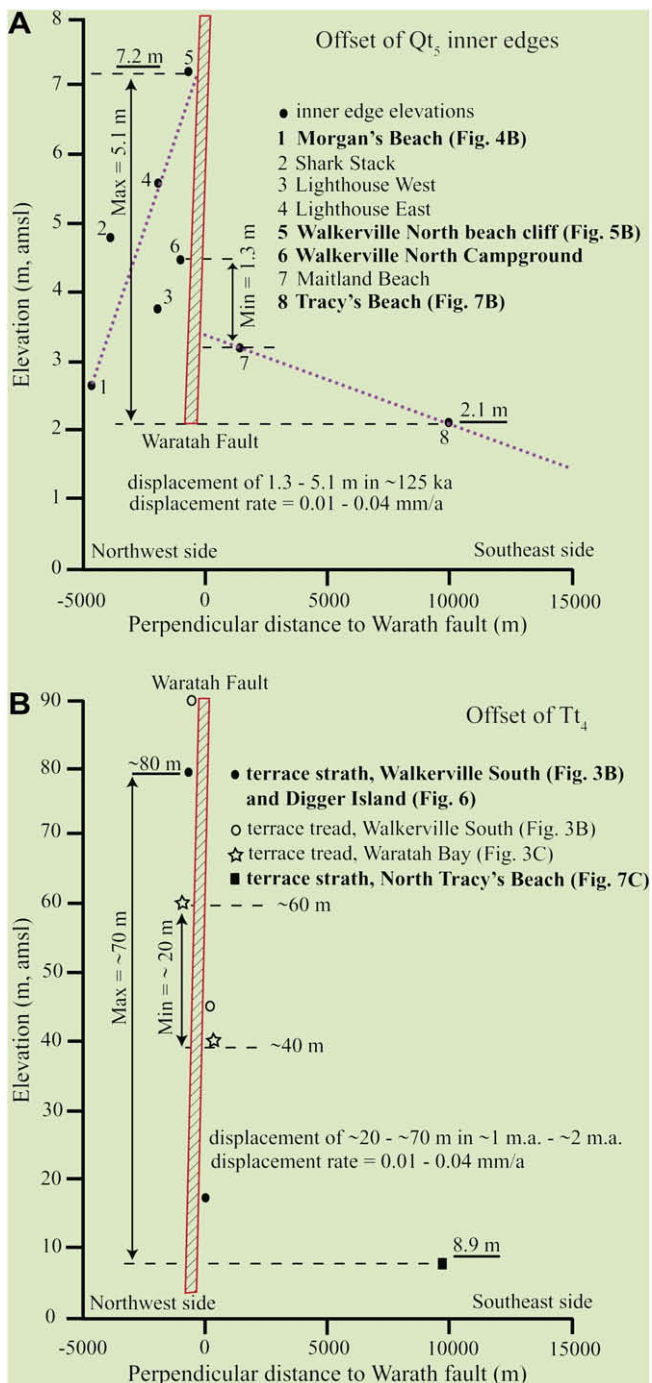


Fig. 8. Terrace displacements across the Waratah Fault. A) Displacement of Qt_5 inner edges across the Waratah Fault. Bold text indicates locations with OSL ages, except for location 1, Morgan's Beach, where the inner edge location (2.1 m amsl) is approximately 100 m southeast of the dated sediment and marine platform (1.2 m amsl) in Fig. 4B. At location 1 the paleo-sea cliff intersects the modern shoreline exposing the inner edge (Gardner et al., 2006). Maximum displacement calculated from difference in elevation of points 5 and 8. Minimum displacement calculated from difference in elevation of points 6 and 7. Fine dashed lines show possible block rotation along the Waratah Fault. Elevations for A were measured with a metric rod and level. B) Displacement of Tt_4 across the Waratah Fault. Bold text indicates locations with CRN ages. Underlined values show highest and lowest inner edge elevations across Waratah Fault. Displacement rate is calculated using a Late Pliocene age, ~2 Ma, for Tt_4 which is the average of the 2 depth corrected burial ages (Table 1). See Fig. 2 for location of all data points.

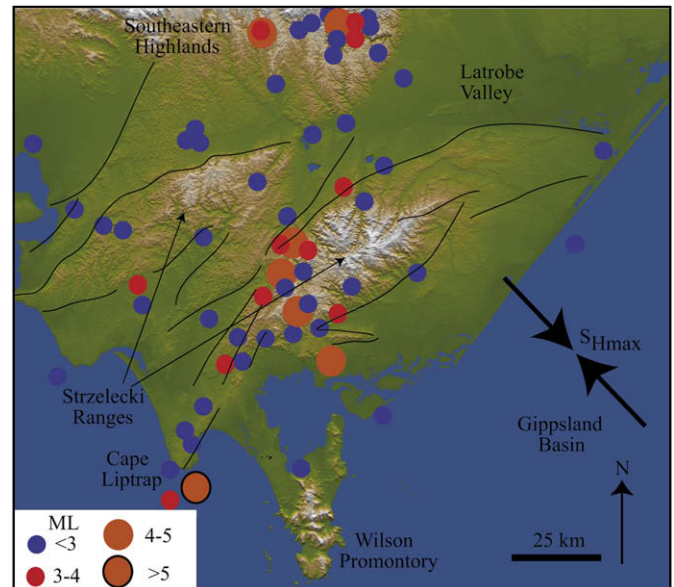


Fig. 9. Distribution of historic seismicity (1859–2000) for Victoria/South Gippsland at the southern end of the Southeastern Australia Seismic Zone (SESZ) as defined by Sandiford and Egholm (2008). Data from Geosciences Australia earthquake database (<http://www.ga.gov.au/map/national/>). See Fig. 1C for location of SESZ. Arrows show average maximum horizontal stress orientation (S_{Hmax}) from Hillis and Reynolds (2003) and Nelson et al. (2006).

Displacement rates of Tt_4 across the Waratah Fault range from 0.01 to 0.04 mm/a using a Late Pliocene (~2 Ma) age for the terrace (Fig. 8B). These estimates are identical to those calculated from Qt_5 , despite the lack of inner edge data for Tt_4 .

Regional tectonic data support these calculated rates of displacement on the Waratah Fault. Seismic strain rates estimated from historic earthquake data for Gippsland would allow for slip of ~0.035 mm/a across a reverse fault dipping at 45° (Sandiford et al., 2003). The Rosedale Fault, a range-bounding fault in the Strzelecki Ranges 75–100 km northeast of Cape Liptrap (Fig. 1A), moved ~60–100 m over the Early to mid-Pleistocene (1.5–0.25 Ma) at a rate of 0.05–0.08 mm/a (Holdgate et al., 2003). In addition, the sense of motion on the Waratah Fault, southeast side down, is consistent with displacement of the Haunted Hill Formation along the Gelliondale Monocline north of Toora (Fig. 1B).

The rate of movement on the Waratah Fault deduced in this study (0.01–0.04 mm/a) falls within the range of calculated slip rates for some faults in stable continental regions (SCR) of Australia (Crone et al., 2003), but well below that for the Lake Edgar Fault in Tasmania (~0.2 mm/a; Clark et al., in press).

4.2. Historic seismicity and the modern stress field

Southeastern Australia has had significant seismic activity over the last 150 years (Gibson et al., 1981; McCue et al., 1990; Sandiford et al., 2003), which has led to identification of the Southeastern Australian Seismic Zone, SESZ (Fig. 1C inset, Sandiford and Egholm, 2008). There is a prominent concentration of earthquakes (return period of ~30 years for magnitude 5.6) in a broad zone from the west coast of Tasmania through Southeastern Australia into New South Wales, with earthquake activity concentrated in the Strzelecki Ranges (McCue et al., 1990; Sandiford, 2002, 2003). This zone (Fig. 9) could have a moment release nearly as great as that of the Flinders Ranges (Sandiford et al., 2003), one of the most seismically active regions in Australia (Célerier et al., 2005). One of the largest earthquakes in Southeastern Australia ($M \sim 5.7$) occurred just offshore of Cape Liptrap on July 2, 1885 (Fig. 9), possibly along the Waratah Fault.

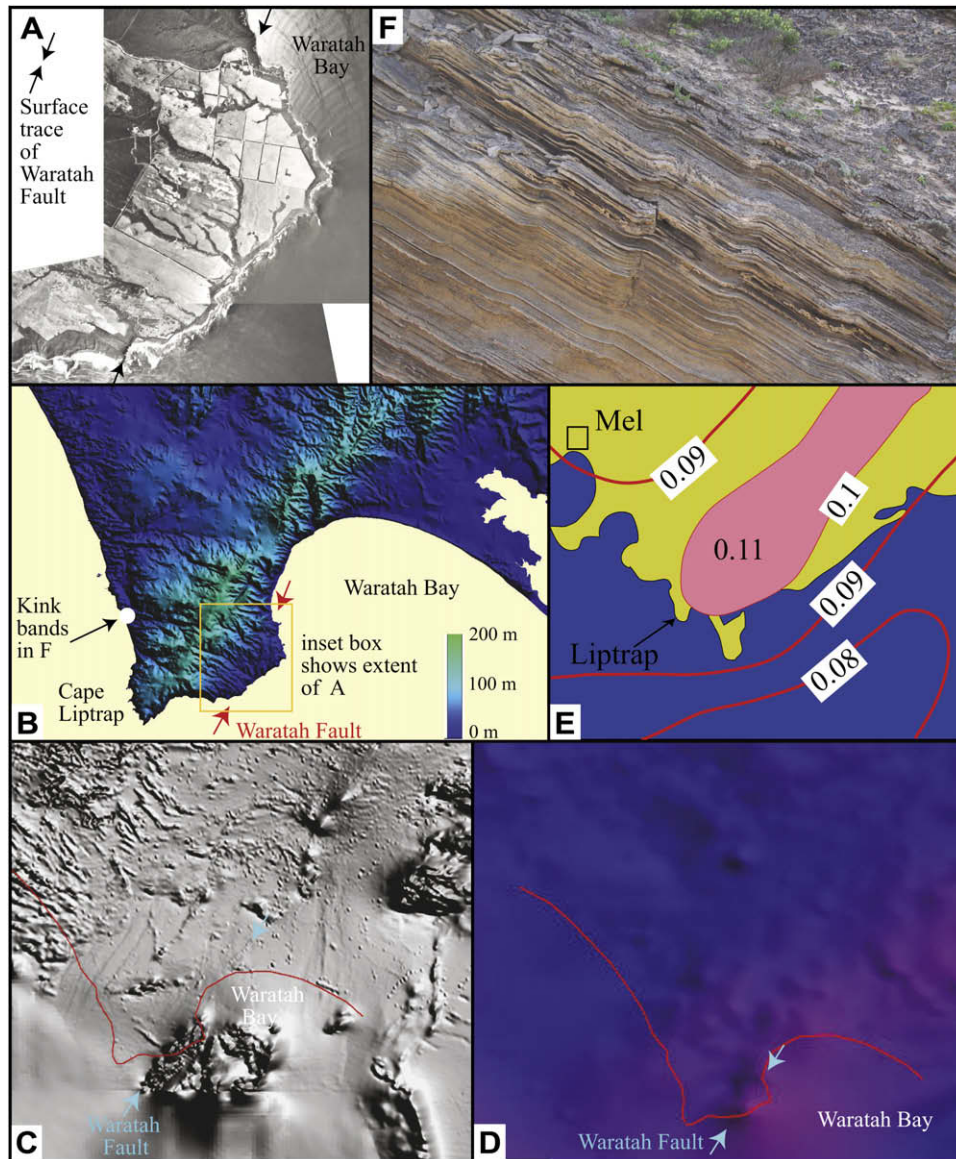


Fig. 10. A) Black and white vertical aerial photograph of Cape Liptrap showing the surface trace of the Waratah Fault, clearly visible on Tt₄ between arrows, but not on the Late Pleistocene dunefields (Fig. 2A). Photographs from QASCO Victoria Pty Ltd, flown in 1985. B) Digital elevation model for Cape Liptrap, showing topographic expression of Waratah Fault. DEM supplied by Land Information Group, Department of Natural Resources and Environment, Victoria; source data sets predominantly at 1:25,000 map scale; x–y resolution 15–30 m, elevation accuracy < 5–10 m. C) Airborne Total Magnetic Intensity (TMI) data for Cape Liptrap Region. Waratah Fault is clearly delineated probably because of juxtaposition of Liptrap Formation turbidites against Early Paleozoic greenstones. TMI image supplied by Geological Survey of Victoria, TMI magnetometer data sampled at rate of 0.1 s, data gridded at 50 m mesh size using a minimum curvature gridding method; pixel shading assigned using histogram equalisation, gradients enhanced with synthetic sun illumination. D) Bouguer gravity anomaly of Cape Liptrap Region showing well defined gravity anomaly along Waratah Fault, again probably reflecting juxtaposition of Liptrap Formation turbidites against denser greenstones. Gravity data supplied by Geological Survey of Victoria, gravity data station spacing varies (mostly 1.5–11 km), data gridded at 300 m mesh size using a minimum curvature gridding method, pixel shading assigned using histogram equalisation, enhanced with synthetic sun illumination. E) Earthquake Hazard Map for the Cape Liptrap Region. Acceleration coefficient [10% chance of being exceeded in 50 years] contours are shown with peak acceleration coefficient value. Modified from Gaull et al. (1990). Mel is Melbourne. F) Kink bands in 70–80 ka aeolianite at Morgan Beach. Field of view is about 6 m². See Fig. 10B for location.

The modern, intraplate stress field in Southeastern Australia (Fig. 9), as determined from petroleum borehole breakouts and focal mechanism solutions from historic earthquakes, is compressional to slightly transpressional (Nelson et al., 2006), with S_{Hmax} -oriented at $130^\circ \pm 20^\circ$ (Hillis and Reynolds, 2003; Sandiford et al., 2004) and is most likely homogeneous between shallow and seismogenic depths (Clark and Leonard, 2003). This broadly NW–SE oriented compressive stress has resulted in reverse motion on some NE–SW striking faults and fault-cored monoclines in the Gippsland Basin (Barton, 1981; Dickinson et al., 2002; Sandiford, 2002; Nelson et al., 2006), so given its orientation, the NE–SW Waratah Fault at Cape Liptrap is also susceptible to reactivation in the modern stress regime.

4.3. History of fault movement

Plate reconstructions indicate that a phase of active deformation across a broad section of the Australian continent began in the Late Miocene (6–8 Ma), attributed to increased compression associated with formation of the Southern Alps of New Zealand along the Australia and Pacific plate boundary (Coblentz et al., 1995, 1998; Sandiford, 2002, 2003; Reynolds et al., 2003; Sandiford et al., 2004; C  lerier et al., 2005; Nelson et al., 2006; Dyksterhuis and M  ller, 2008), and has been ongoing with variable intensity into the present. For example, recent reactivation of faults has been documented in the Flinders Ranges in South Australia (C  lerier et al., 2006; Quigley et al., 2006). This phase of active deformation is

generally consistent with the modern, intraplate stress field in Southeastern Australia (Sandiford, 2003; Sandiford and Egholm, 2008).

In western Victoria this period of tectonism displaced Late Miocene strandlines but not the overlying 4 Ma basalts (Paine et al., 2004), and in the Gippsland Basin it formed an angular unconformity between the Pliocene Jemmy Point Formation and the overlying alluvial Pliocene Haunted Hill Formation (Bolger, 1991; Dickinson et al., 2002; Wallace et al., 2005). From an analysis of Pliocene and Quaternary strandlines in southern Victoria, Wallace et al. (2005) inferred reduced rates of tectonism in the Pliocene that accelerated in the Quaternary. Holdgate et al. (2003) concluded that tectonism in the offshore Gippsland Basin slowed post-1 Ma, but continued onshore to 0.2 Ma. Our analysis of movement along the Waratah Fault suggests that active deformation began in the Neogene, at least by the Late Pliocene (Tt₄), and has been ongoing at similar time-averaged rates.

However, fault activity during this time has been episodic, as is the case for many active faults in stable continental regions (Crone et al., 1997, 2003). The different sediment thicknesses for Tt₄ on either side of the Waratah Fault at Walkerville South (Fig. 3B) most likely reflect syndepositional fault movement, as previously discussed, so faulting was especially active during deposition of these sediments during the sea level highstand in the Late Pliocene. The most recent movement on the Waratah Fault displaced the Late Pleistocene Qt₅ terrace (which formed at 125 ± 5 ka), and kinked calcareous aeolinites (Sandiford, 2003) at Morgan's Beach (Fig. 2A) dated at 70–80 ka (Gardner et al., 2006), and is responsible for the high visibility of the fault on air photographs and the digital elevation model of the area (Fig. 10A and B). The latest Pleistocene (19–25 ka) dunefields (Gardner et al., 2006) that cover Tt₄ and Qt₅ across the Waratah Fault show no evidence of fault offset, although it would be difficult to preserve fault scarps on unconsolidated dune sands. However, the mid-Holocene terrace, Qt₆, has not been displaced.

4.4. Triggering of fault movement

The Waratah Fault is susceptible to movement in the modern stress field due to its favorable orientation (Fig. 9), a condition noted for other active faults in intraplate settings (Crone et al., 1997). In addition, it lies 100–200 km inboard of the ocean-continent lithosphere transition, where thermal effects from lateral heat flow can substantially elevate strain rates relative to continental interiors (Sandiford and Egholm, 2008). Furthermore, the Waratah fault separates rock units of very different magnetic and gravity signatures (Fig. 10C, D), with Paleozoic sedimentary rocks to the west and probably greenstones to the east. Rapid variations in material strength across fault boundaries can increase the likelihood of movement (Clark et al., in press; Dentith and Featherstone, 2003).

A major episode of movement on the Waratah Fault in the Late Pliocene coincides with a eustatic sea level highstand, and it is possible that high sea levels trigger fault activity. Given the position of the Waratah Fault relative to the modern coast (Figs. 1 and 2), during sea level highstands the southeast side is loaded preferentially, and pore pressures within the cataclastic zone of the fault, which is several 10s of metres wide, would increase, particularly offshore. Clark et al. (in press) suggest that increased pore pressure from higher groundwater tables during climatically optimal conditions could trigger episodic movement on the Lake Edgar Fault in Tasmania.

Following this reasoning, the latest phase of major fault activity could have coincided with the rise in sea level following the Last Glacial Maximum; this period of movement occurred after 70–80 ka and prior to the mid-Holocene, as discussed above.

The Waratah Fault may have moved episodically during all sea level highstands since the Late Pliocene, because the time-averaged

rates for the Late Pliocene are identical to those for the Late Pleistocene. This suggests that intervals between major seismic events are of the order of 100 ka, somewhat longer than suggested for SCR faults in Western Australia, South Australia and the Northern Territory (Crone et al., 1997, 2003)

4.5. Implications for seismic risk

Cape Liptrap lies within the southwestern part of the Southeastern Australian Seismic Zone, with peak ground acceleration coefficients estimated to be around 0.11 (Fig. 10E). The severity of ground shaking during a seismic event along the fault is indicated by the deformation of calcarenite dune sands at Morgan's Beach (Fig. 10F), ~6 km from the fault trace. Depending upon the degree of lithification of these dune sands, ground acceleration coefficients could have been well above those predicted from the seismic hazard map for the area (Gauil et al., 1990). This implies a considerable degree of seismic risk for the Cape Liptrap Region.

Interseismic intervals for periods of major activity on the fault may be of the order of 100 ka if they are controlled by eustatic sea level highstands, with the youngest substantial movement perhaps ~20,000 years ago. Nevertheless, historical earthquakes of magnitude 5–6 have been recorded in the area, indicating ongoing seismic activity.

5. Conclusions

The Waratah Fault is a northeast trending, high angle, reverse fault in the Late Paleozoic Lachlan Fold Belt at Cape Liptrap on the Southeastern Australian coast. It forms a prominent structural boundary in the Lachlan Fold Belt discernible from airborne magnetic and bouger gravity anomalies. Relative to the modern, intraplate stress field in southeast Australia, the fault is susceptible to reactivation. It is in the southwestern corner of the SESZ with one of the largest earthquakes in Southeastern Australia of M ~5.7 occurring just offshore on July 2, 1885. A flight of six marine terraces occur on Cape Liptrap from an elevation of ~1.5 m amsl to ~170 m amsl. Terrace ages range from mid-Holocene to Neogene. The ages of the lowest three terraces are constrained by radiocarbon, OSL and CRN dating. Qt₆, the lowest terrace is mid-Holocene, 5220 ± 50 years BP. Four OSL ages from Qt₅ constrain that terrace to the Last Interglacial sea level highstand (MIS 5e) at ~125 ka. Depth corrected CRN burial ages constrain Tt₄ to the Late Pliocene. The ages of the highest three terraces, Tt₃–Tt₁, are broadly assigned to global sea level highstands during the Neogene.

Displacement rates across the Waratah Fault range from 0.01 mm/a to 0.04 mm/a for Qt₅. Displacement rates range from 0.01 to 0.04 mm/a for Tt₄. These calculated rates are consistent with rates estimated from other diverse tectonic data sets around the Gippsland Basin and from numerical modeling. Our analysis of movement along the Waratah Fault suggests that active deformation began at least by the Late Pliocene (the oldest cosmogenic ages for Tt₄) and has been ongoing at least into the latest Pleistocene (Qt₅) at similar time-averaged rates.

Seismicity and deformation are episodic. Episodic movement on the Waratah Fault may be coincident with sea level highstands since the Late Pliocene, possibly from increased loading and elevated pore pressure within the fault zone.

Acknowledgements

We thank J. Bowler, M. Orr, M. Sandiford, and A. Vandenberg for stimulating discussions in the field, Heather and David Bligh of the Toora Tourist Park for logistical support, and Tony and Elizabeth Landy and other local residents for critical land access. Barton

Smith provided the Qt5-OSL-4 age. The Keck Geology Consortium provided financial support.

References

- Adamec, G., Aitken, M.J., 1998. Dose-rate conversion factors: update. *Ancient TL* 16, 37–50.
- Anderson, R.S., Densmore, A.L., Ellis, M.A., 1999. The generation and degradation of marine terraces. *Basin Research* 11, 7–19.
- Andrews, E., 1910. Geographical unity of eastern Australia in late and post Tertiary time with applications to biological problems. *Journal and Proceedings of the Royal Society of New South Wales* 44, 420–480.
- Baker, R.G.V., Haworth, R.J., Flood, P.G., 2001. Warmer or cooler Late Holocene marine paleoenvironments? Interpreting southeast Australian and Brazilian sea-level changes using fixed biological indicators and their $\delta^{18}\text{O}$ composition. *Palaeogeography, Palaeoclimatology, Palaeoecology* 168, 249–272.
- Barton, C., 1981. Regional stress and structure in relation to brown coal open pits cuts of the Latrobe Valley. *Journal of the Geological Society of Australia* 28, 333–340.
- Beaman, R., Larcombe, Carter, R.M., 1994. New evidence for the Holocene sea-level high from the inner shelf, central Great Barrier Reef, Australia. *Journal of Sedimentary Research* A64, 881–885.
- Belperio, A.P., Harvey, N., Bourman, R.P., 2002. Spatial and temporal variability in the Holocene sea-level record of the South Australian coastline. *Sedimentary Geology* 150, 153–169.
- Bishop, P., 1998. Griffith Taylor and the SE Australian Highlands: issues of data sources and testability in interpretations of long-term drainage history and landscape evolution. *Australian Geographer* 29, 7–29.
- Bolger, P.F., 1991. Lithofacies variations as a consequence of Late Cainozoic tectonic and paleoclimatic events in the onshore Gippsland Basin. In: Williams, M.A.J., de Deckker, P., Kershaw, A.P. (Eds.), *The Cainozoic in Australia: a Re-appraisal of the Evidence*. Geological Society of Australia, Special Publications, vol. 18, pp. 158–180.
- Bourman, R.P., Lindsay, J.M., 1989. Timing, extent and character of Late Cainozoic faulting on the eastern margin of the Mt Lofty Ranges, South Australia. *Transactions of the Royal Society of South Australia* 113, 63–67.
- Bourman, R.P., Belperio, A.P., Murray-Wallace, C.V., Cann, J.H., 1999. A Last Glacial embayment fill at Normanville, South Australia, and its neotectonic implications. *Transactions of the Royal Society of South Australia* 123, 1–15.
- Bradley, W., Griggs, G., 1976. Form, genesis, and deformation of central California wave-cut platforms. *Geological Society of America Bulletin* 87, 433–449.
- C  lerier, J., Sandiford, M., Hansen, D.L., Quigley, M., 2005. Modes of active intraplate deformation, Flinders Ranges, Australia. *Tectonics* 24, TC6006. doi:10.1029/2004TC001679.
- Chappell, J., 1983. Evidence for smoothly falling sea level relative to north Queensland, Australia, during the past 6000 yr. *Nature* 302, 406–408.
- Clark, D., Leonard, M., 2003. Principal stress orientations from multiple focal-plane solutions: new insights into the Australian intraplate stress field. In: Hillis, R.R., M  ller, R.D. (Eds.), *Evolution and Dynamics of the Australian Plate*. Geological Society of America, Special Publication, vol. 372, pp. 49–58.
- Clark, D., Cupper, M., Sandiford, M., Kiernan, K. Style and Timing of Late Quaternary Faulting in the Lake Edgar Fault, Southwest Tasmania: Implications for Hazard Assessment in Intracontinental Areas. Geological Society of America, Special Publication, Paleoseismicity, in press.
- Coblentz, D.D., Sandiford, M., Richardson, R.M., Zhou, S., Hillis, R.R., 1995. The origins of the intraplate stress field in continental Australia. *Earth and Planetary Science Letters* 133, 299–309.
- Coblentz, D.D., Zhou, S., Hillis, R.R., Richardson, R.M., Sandiford, M., 1998. Topography, boundary forces, and the Indo-Australian intraplate stress field. *Journal of Geophysical Research* 103, 919–931.
- Cooper, F., Roberts, G., Underwood, C., 2007. A comparison of 10^3 – 10^5 year uplift rates on the South Alkyonides Fault, central Greece: Holocene climate stability and the formation of coastal notches. *Geophysical Research Letters* 34, L14310. doi:10.1029/2007GL030673.
- Crone, A.J., Machette, M.N., 1994. Paleoseismology of Quaternary faults in the “stable” interior of Australia and North America – insights into the long-term behavior of seismogenic faults. In: Prentice, C.S., Schwartz, D.P., Yeats, R.S. (Eds.), *Proceedings of the Workshop on Paleoseismicity*, United States Geological Survey Open File Report 94-568, 210 pp.
- Crone, A.J., Machette, M.N., Bowman, J.R., 1997. Episodic nature of earthquake activity in stable continental regions revealed by palaeoseismicity studies of Australia and North American Quaternary faults. *Australian Journal of Earth Sciences* 44, 203–214.
- Crone, A.J., De Martini, P.M., Machette, M.N., Okumura, K., Prescott, J.R., 2003. Paleoseismicity of two historically quiescent faults in Australia: implications for fault behavior in stable continental regions. *Bulletin of the Seismological Society of America* 93, 1913–1934.
- Cupper, M.L., 2006. Luminescence and radiocarbon chronologies of playa sedimentation in the Murray Basin, southeastern Australia. *Quaternary Science Reviews* 25, 2594–2607.
- Dentith, M.C., Featherstone, W.E., 2003. Controls on intra-plate seismicity in southwestern Australia. *Tectonophysics* 376, 167–184.
- Dickinson, J.A., Wallace, M.W., Holdgate, G.R., Gallagher, S.J., Thomas, L., 2002. Origin and timing of the Miocene–Pliocene unconformity in southeast Australia. *Journal of Sedimentary Petrology* 72, 288–303.
- Douglas, J.G., 1972. Sale, S.J. 55–11, first ed. In: Geological Map Series Department of Natural Resources and Environment, Victoria. Scale 1:250,000.
- Douglas, J.G., 1975. Liptrap and Part of the Yanakie. Geological Survey of Victoria, Melbourne. Parts 8020 and 8120, Zone 55, Scale 1:63,360.
- Douglas, J.G., 1993. Victoria Geologic Map. Geological Survey of Victoria, Melbourne. Scale 1:1,000,000.
- Douglas, J.G., Spencer-Jones, D., 1971. Warragul, S.J55–10, first ed. In: Geological Map Series Geological Society of Victoria. Scale 1:250,000.
- Dowsett, H.J., Cronin, T.M., 1990. High eustatic sea level during the middle Pliocene: evidence from the southeastern U.S. Atlantic Coastal Plain. *Geology* 18, 435–438.
- Dyksterhuis, S., M  ller, R.D., 2008. Cause and evolution of intraplate orogeny in Australia. *Geology* 36, 495–498.
- Fink, D., Hotchkis, M., Hua, Q., Jacobsen, G., Smith, A.M., Zoppi, U., Child, D., Mifsud, C., van der Gaast, H., Williams, A., Williams, M., 2004. The ANTARES AMS facility at ANSTO. *Nuclear Instruments & Methods in Physics Research B223–B224*, 109–115.
- Fischer, R., 1980. Recent tectonic movements of the Costa Rican Pacific coast. *Tectonophysics* 70, T25–T33.
- Gardner, T., Marshall, J., Merritts, D., Bee, B., Burgette, R., Burton, E., Cooke, J., Kehrwald, N., Protti, M., Fisher, D., Sak, P., 2001. Holocene forearc deformation in response to seamount subduction, Peninsula de Nicoya, Costa Rica. *Geology* 29, 151–154.
- Gardner, T., Webb, J., Davis, A., Cassel, E., Pezzia, C., Merritts, D., Smith, B., 2006. Late Pleistocene landscape response to climate change: eolian and alluvial fan deposition, Cape Liptrap, southeastern Australia. *Quaternary Science Reviews* 25, 1552–1569. doi:10.1016/j.quascirev.2005.12.003.
- Gaull, B.A., Michael-Leiba, M.O., Rynn, J.M.W., 1990. Probabilistic earthquake risk maps of Australia. *Australian Journal of Earth Sciences* 37, 169–187.
- Geological Survey of Victoria, 1993. Victoria Geological Map. Geological Survey of Victoria, Melbourne. Scale 1:1,000,000.
- Geosciences Australia, 2008. Online Earthquake Database Available from: <http://www.ga.gov.au/oracle/quake/quake_online.jsp>.
- Gibson, G., Wesson, V., Cuthbertson, R., 1981. Seismicity of Victoria to 1980. *Journal of the Geological Society of Australia* 28, 341–356.
- Goy, J.L., Machare, J., Ortlieb, L., Zazo, C., 1992. Quaternary shorelines in southern Peru: a record of global sea-level fluctuations and tectonic uplift in Chala Bay. *Quaternary International* 15, 99–112.
- Granger, D.E., Muzikar, P.F., 2001. Dating sediment burial with in situ-produced cosmogenic nuclides: theory, techniques, and limitations. *Earth and Planetary Science Letters* 188, 269–281.
- Gray, D., 1988. Structure and tectonics. In: Douglas, J.G., Ferguson, J.A. (Eds.), *Geology of Victoria*. Victoria Division, Geological Society of Australia, Melbourne, pp. 1–36.
- Haq, B.U., Hardenbol, J., Vail, P.R., 1987. Chronology of fluctuating sea levels since the Triassic. *Science* 235, 1156–1167.
- Haworth, R.J., Baker, R.G.V., Flood, P.G., 2002. Predicted and observed Holocene sea-levels on the Australian coast; what do they indicate about hydro-isostatic models in far-field sites? *Journal of Quaternary Science* 17, 581–591.
- Hillis, R.R., Reynolds, S.D., 2003. *In situ* stress field of Australia. In: Hillis, R.R., M  ller, R.D. (Eds.), *Evolution and Dynamics of the Australian Plate*. Geological Society of America, Special Publication, vol. 372, pp. 49–58.
- Hocking, J., 1988. Gippsland Basin. In: Douglas, J.G., Ferguson, J.A. (Eds.), *Geology of Victoria*. Victoria Division, Geological Society of Australia, Melbourne, pp. 322–347.
- Holdgate, G.R., Wallace, M.W., Gallagher, S.J., Smith, A.J., Keene, J.B., Moore, D., Shafik, S., 2003. Plio-Pleistocene tectonics and eustasy in the Gippsland Basin, southeast Australia: evidence from magnetic imagery and marine geology. *Australian Journal of Earth Sciences* 50, 403–426.
- Jenkin, J.J., 1968. The Geomorphology and Upper Cainozoic Geology of South-east Gippsland, Victoria. Geological Survey of Victoria Memoir 27, 152.
- Jenkin, J.J., 1981. Evolution of the Victorian coastline. *Proceedings of the Royal Society of Victoria* 99, 37–54.
- Jenkin, J.J., 1988. Westport and Southern Gippsland. In: Douglas, J.G., Ferguson, J.A. (Eds.), *Geology of Victoria*. Victoria Division, Geological Society of Australia, Melbourne, pp. 392–402.
- Joyce, E.B., Webb, J.A., et al., 2003. Chapter 18 – geomorphology. In: Birch, W. (Ed.), *Geology of Victoria*. Geological Society of Australia, Special Publication, vol. 23, pp. 533–561.
- Kershaw, S., Guo, L., 2001. Marine notches in coastal cliffs: indicators of relative sea level change, Perachora Peninsula, central Greece. *Marine Geology* 179, 213–228.
- Kominz, M.A., Miller, K.G., Browning, J.V., 1998. Long-term and short-term global Cenozoic sea-level estimates. *Geology* 26, 311–314.
- Kotsonis, A., 1996. Late Cainozoic climate and eustatic record of the Loxton-Parilla Sands, Murray Basin southeastern Australia. MSc thesis, University of Melbourne, Melbourne, Victoria, 152 pp.
- Lajoie, K.R., 1986. Coastal tectonics. In: Wallace, R.E. (Ed.), *Active Tectonics*. Studies in Geophysics Series. National Academy Press, Washington, D.C., pp. 95–124.
- McCue, K., Gibson, G., Wesson, V., 1990. The earthquake near Nhill, western Victoria, on 22 December 1987 and the seismicity of eastern Australia. *BMR Journal of Australian Geology and Geophysics* 11, 415–420.
- Merritts, D., 1996. The Mendicino triple junction: active faults, episodic coastal emergence, and rapid uplift. *Journal of Geophysical Research* 101, 6051–6070.
- Muhs, D.R., 2002. Evidence for the timing and duration of the Last Interglacial period from high-precision uranium-series ages of coral on tectonically stable coastlines. *Quaternary Research* 58, 36–40.

- Murray, A.S., Roberts, R.G., 1998. Measurement of the equivalent dose in quartz using a regenerative-dose single-aliquot protocol. *Radiation Measurements* 29, 503–515.
- Murray, A.S., Wintle, A.G., 2000. Luminescence dating of quartz using an improved single-aliquot regenerative-dose protocol. *Radiation Measurements* 32, 57–73.
- Murray-Wallace, C.V., 2002. Pleistocene coastal stratigraphy, sea-level highstands and neotectonism of the southern Australian passive continental margin – a review. *Journal of Quaternary Science* 17, 469–489.
- Murray-Wallace, C.V., Belperio, A.P., 1991. The Last Interglacial shoreline in Australia – a review. *Quaternary Science Reviews* 10, 441–461.
- Murray-Wallace, C.V., Belperio, A.P., Cann, J.H., Huntley, D.J., Prescott, J.R., 1996. Late Quaternary uplift history, Mount Gambier region, South Australia. *Zeitschrift für Geomorphologie N.F. Suppl.* 106, 41–56.
- Nelson, E., Hillis, R., Sandiford, M., Reynolds, S., Mildren, S., 2006. Present-day state of stress of southeast Australia. *Australian Petroleum Production & Exploration Association Journal*, 283–305.
- Ollier, C.D., 1978. Tectonics and geomorphology of the Eastern Highlands. In: Davies, J.L., Williams, M.J. (Eds.), *Landform Evolution in Australasia*. Australia National University Press, Canberra, pp. 5–47.
- Ollier, C.D., Pain, C.F., 1994. Landscape evolution and tectonics in southeastern Australia. *AGSO Journal of Australian Geology & Geophysics* 15, 335–345.
- Paine, M., Bennetts, D.A., Webb, J.A., Morand, V., 2004. Nature and extent of Pliocene strandlines in southwestern Victoria and their application to Late Neogene tectonics. *Australian Journal of Earth Sciences* 51, 407–422.
- Pazzaglia, F.J., Gardner, T.W., 1993. Fluvial terraces of the lower Susquehanna River. *Geomorphology* 8, 83–113.
- Perg, L.A., Anderson, R.S., Finkel, R.C., 2001. Use of a new Be-10 and Al-26 inventory method to date marine terraces, Santa Cruz, California, USA. *Geology* 29, 879–882.
- Prescott, J.R., Hutton, J.T., 1994. Cosmic ray contributions to dose rates for luminescence and ESR dating: large depths and long term variations. *Radiation Measurements* 23, 497–500.
- Quigley, M., Cupper, M.L., Sandiford, M., 2006. Quaternary faults of south-central Australia: palaeoseismicity, slip rates and origin. *Australian Journal of Earth Sciences* 53, 285–301.
- Quigley, M., Sandiford, M., Fifield, L.K., Alimanovic, A., 2007. Landscape response to intraplate tectonism: quantitative constraints from ¹⁰Be nuclide abundances. *Earth and Planetary Sciences Letters* 261, 120–133.
- Reynolds, S.D., Coblenz, D.D., Hillis, R.R., 2003. Influences of plate-boundary forces on the regional intraplate stress field of continental Australia. In: Hillis, R.R., Müller, R.D. (Eds.), *Evolution and Dynamics of the Australian Plate*. Geological Society of America, Special Publication, vol. 372, pp. 59–70.
- Sandiford, M., 1978. The geology of Waratah Bay axis: late diagenetic/tectonic structures in the Devonian limestones of Waratah Bay. BSc thesis (Honours), University of Melbourne, Melbourne, Victoria, 58 pp.
- Sandiford, M., 2002. Late Neogene faulting record in Southeastern Australia. In: Phillips, G.N., Ely, K.S. (Eds.), *Victoria Undercover*, pp. 131–135.
- Sandiford, M., 2003. Neotectonics of Southeastern Australia: linking the Quaternary faulting record with seismicity and *in situ* stress. In: Hillis, R.R., Müller, R.D. (Eds.), *Evolution and Dynamics of the Australian Plate*. Geological Society of America, Special Publication, vol. 372, pp. 107–119.
- Sandiford, M., Leonard, M., Coblenz, D., 2003. Geological constraints on active seismicity in southeast Australia. In: Wilson, J.L., Lam, N.K., Gibson, G. (Eds.), *Earthquake Risk Mitigation*. Australian Earthquake Engineering Society, pp. 1–10.
- Sandiford, M., Wallace, M., Coblenz, D., 2004. Origin of the *in situ* stress field in south-eastern Australia. *Basin Research* 16, 325–338.
- Sandiford, M., Egholm, D.L., 2008. Enhanced intraplate seismicity along continental margins: some causes and consequences. *Tectonophysics* 457, 197–208.
- Sprigg, R.C., 1979. Stranded and submerged sea-beach systems of southeast South Australia and the aeolian desert cycle. *Sedimentary Geology* 22, 53–96.
- Stirling, C.H., Esat, T.M., Lambeck, K., McCulloch, M.T., 1998. Timing and duration of the Last Interglacial: evidence for a restricted interval of widespread coral reef growth. *Earth and Planetary Science Letters* 160, 745–762.
- Stone, J.O., 2000. Air pressure and cosmogenic isotope production. *Journal of Geophysical Research* 105 (B10), 23753–23759.
- Thom, B.G., Roy, P.S., 1985. Relative sea levels and coastal sedimentation in southeast Australia in the Holocene. *Journal of Sedimentary Petrology* 55, 257–264.
- Twidale, C.R., 1983. Australian laterites and silcretes – ages and significance. *Revue de Géologie Dynamique et de Géographie Physique* 24, 35–45.
- VandenBerg, A.H.M., 1977. Bairnsdale, SJ 55-7, first ed.. In: *Geological Map Series* Department of Natural Resources and Environment, Victoria. Scale 1:250,000.
- VandenBerg, A.H.M., 1997. Warragul, SJ 55-10, second ed.. In: *Geological Map Series* Department of Natural Resources and Environment, Victoria. Scale 1:250,000.
- VandenBerg, A.H.M., 1988. Silurian-middle Devonian. In: Douglas, J.G., Ferguson, J.A. (Eds.), *Geology of Victoria*. Victoria Division, Geological Society of Australia, Melbourne, pp. 103–146.
- Wallace, M.W., Dickinson, J.A., Moore, D.H., Sandiford, M., 2005. Late Neogene strandlines of southern Victoria: a unique record of eustasy and tectonics in southeast Australia. *Australian Journal of Earth Sciences* 52, 277–295.
- Ward, W.T., 1985. Correlation of east Australian Pleistocene shorelines with deep-sea core stages: a basis for a coastal chronology. *Geological Society of America Bulletin* 96, 1156–1166.
- Ward, W.T., Ross, P.J., Colquhoun, D.J., 1971. Interglacial high sea levels – an absolute chronology derived from shoreline elevations. *Palaeogeography, Palaeoclimatology, Palaeoecology* 9, 77–99.
- Young, R.W., Bryant, E.A., 1993. Coastal rock platforms and ramps of Pleistocene and Tertiary age in Southern New South Wales, Australia. *Zeitschrift für Geomorphologie N.F.* 37, 257–272.